Cognitive Radio and TV White Space (TVWS) Applications

Book Section

Cognitive Radio and TV White Space (TVWS) Applications

J. H. Martin FIET[1/2], L. S. Dooley[2], K. C. P. Wong MIET[2]

[1]Nokia, 740 Waterside Drive, Aztec West, Bristol, BS32 4UF, United Kingdom

[2] School of Computing and Communications, The Open University, Milton Keynes, MK7 6AA, United Kingdom

---

Contents

Abstract

As more user applications emerge for wireless devices, the corresponding amount of traffic is rapidly expanding, with the corollary that ever-greater spectrum capacity is required. Service providers are experiencing deployment blockages due to insufficient bandwidth being available to accommodate such devices. *TV White Space* (TVWS) represents an opportunity to supplement existing licensed spectrum by exploiting unlicensed resources. TVWS spectrum has materialised from the unused TV channels in the switchover from analogue to digital platforms. The main obstacles to TVWS adoption are reliable detection of *primary users* (PU) i.e., TV operators and consumers, allied with specifically, the *hidden node* problem. This chapter presents a new *Generalised Enhanced Detection Algorithm* (GEDA) that exploits the unique way *Digital Terrestrial TV* (DTT) channels are deployed in different geographical areas. GEDA effectively transforms an energy detector into a feature sensor to achieve significant improvements in detection probability of a DTT PU. Furthermore, by framing a novel margin strategy utilising a *keep out contour*, the hidden node issue is resolved, and a

viable secondary user sensing solution formulated. Experimental results for a cognitive radio TVWS model have formalised both the bandwidth and throughput gains secured by TVWS users with this new paradigm.

---

1. Introduction

Mobile communications have become integral to our daily lives with the mobile phone now having developed into a smart device that is able to interact with its user. Commensurately, mobile data traffic has grown exponentially due to a vast array of services and applications for smartphones including interactive gaming, video and music streaming, web-browsing and e-mail [1, 2].

In many countries, terrestrial TV broadcast networks are changing from analogue to digital delivery platforms, a process already completed in North America, the UK and Europe [3, 4]. This switchover process has continued apace because during migration, maintenance updates were necessary to channel allocations, with the most recent respectively being in 2016 and 2015 for the UK [5] and USA [6]. The switchover released valuable spectrum in the UHF band which was subsequently split into two categories. The first, known as the *Digital Dividend*, denoted spectrum no longer used by terrestrial TV broadcast networks. This was auctioned for mobile operators to develop application technologies like *Long-Term Evolution* (LTE) [3, 4]. The second, known as *TV White Space* (TVWS) or interleaved spectrum, relates to unused spectrum within given geographical locations that avoids adjacent and co-channel interference with *digital terrestrial TV* (DTT) transmitters. Since the *Digital Dividend* spectrum has already been sold off, TVWS has come to be the primary spectrum for *cognitive radio network* (CRN) services and applications.

With 5G mobile technology evolving, there are two nascent views for how it will be successfully realised: i) a focus on greater coverage [7, 8, 9] and ii) increasing throughput and lower latency [7, 8, 9]. The emergence of CRN technology [2, 10, 11] and TVWS provides new access opportunities for unlicensed *secondary users* (SU), and since TVWS exists in the low UHF band, it offers greater coverage and increased throughput so satisfying a major 5G requirement. This chapter presents a framework for how TVWS can effectively fulfil the aforementioned 5G criteria allowing services to not only exploit the increased spectrum released by TVWS, but also ensure long-term SU access benefits, especially as bandwidth scarcity is still a major 5G issue [5, 6].

2. Sensing Strategies

CRN offers an efficient and autonomous TVWS solution to facilitate SU access by sensing the RF environment within licensed *primary user* (PU) spectrum **[**12, 13]. Since TVWS is static spectrum, channels do not change in a particular location so relaxing the need for efficient PU updates as channels vary only on a spatial not temporal basis [12, 14]. To access unused TVWS, *spectral holes* [10, 11] must be identified using *dynamic spectrum access* (DSA) techniques [10, 14) which enable the CRN to learn about its neighbouring RF environment and make access decisions accordingly. DSA techniques for TVWS are generally classified into three categories: beacons, sensing and static databases [12, 13].

Beacons are dedicated in-band signals that advertise for SU access in the licensed spectrum, though since the PU must administer this process, it is not practical for DTT broadcasters due to the prohibitive overheads incurred.

Sensing techniques in contrast, automatically update a PU static database to reduce operational costs, though the ubiquitous *hidden node* problem [4] must be overcome for them to be viable.

Static databases require manual upkeep but as interference margins for PU protection are theoretically calculated rather than based on actual measurements, system accuracy can be compromised. This approach offers greater flexibility in embracing scenarios where sensing is not feasible, such as *programme making and special event* (PMSE) radio microphones.

The principal requirement for TVWS access is reliable PU detection to avoid interference to local DTT users. Both Ofcom and FCC favour the geo-location database approach [12], though this entails expense to implement and maintain the database infrastructure. It is for these reasons that alternative sensing mechanisms are considered in this chapter. Another key sensing issue to resolve is the *hidden node* problem [11, 15, 16], where a SU sensing receiver is obstructed from a PU transmitter, so a spectral hole is falsely detected, potentially causing major PU disruption. This is especially critical at the cell edge where signal strength is generally low.

While assorted co-operative sensing solutions exist [17] to overcome hidden nodes, the novel GEDA solution presented in this chapter, does not rely on either co-operative mechanisms or compromises SU bandwidth availability. It exploits the unique deployment pattern of DTT frequencies to determine if a PU channel is occupied, applying an energy detector for local real-time measurements in the decision making, so effectively turning it into a feature detector. We will now investigate in greater depth the rich opportunity TVWS spectrum affords for providing extra bandwidth for SU access.

3. TV White Space (TVWS)

The DTT switchover from analogue TV reduced the number of TV channels, with some being released for auction, while the remainder were allocated as DTT channels. Unused DTT channels in a particular geographic area is TVWS (interleaved spectrum) and in the most recent standards [5, 6] are assigned to CRN applications. The UK 8MHz DTT channels are shown in Figure 1, with TVWS channels being the unused (interleaved) spectrum in any location. The purple channels are DTT, green channels have been auctioned and the pink channel is for PMSE applications.

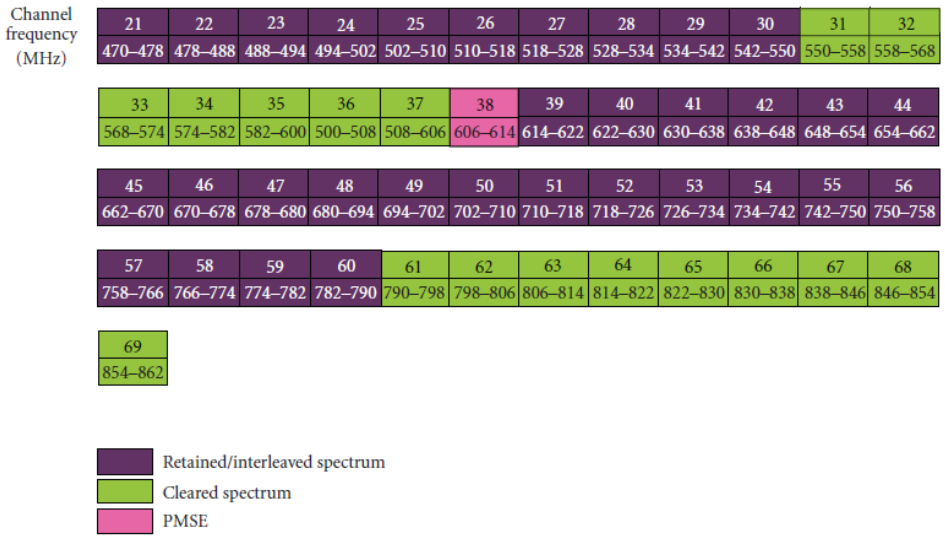

Figure 1: Channel allocation after DTT conversion in the UK [5]

In [3], it was noted that in the UK, 50% of locations can release 150 MHz of spectrum and from 90% of locations, 100 MHz of TVWS. The key issue distilled from this analysis is that for a CRN to utilise TVWS it must be able to allocate non-contiguous channels to all its SU. Figure 2 shows the non-contiguous nature of channels allocated in London, where each cyan bar represents a free 8MHz channel. It is evident the maximum contiguous channel capacity is

16MHz i.e., 2 adjacent cyan bars, so to achieve greater capacity non-contiguous techniques such as assembly and disassembly of non-contiguous OFDM channels must be employed.

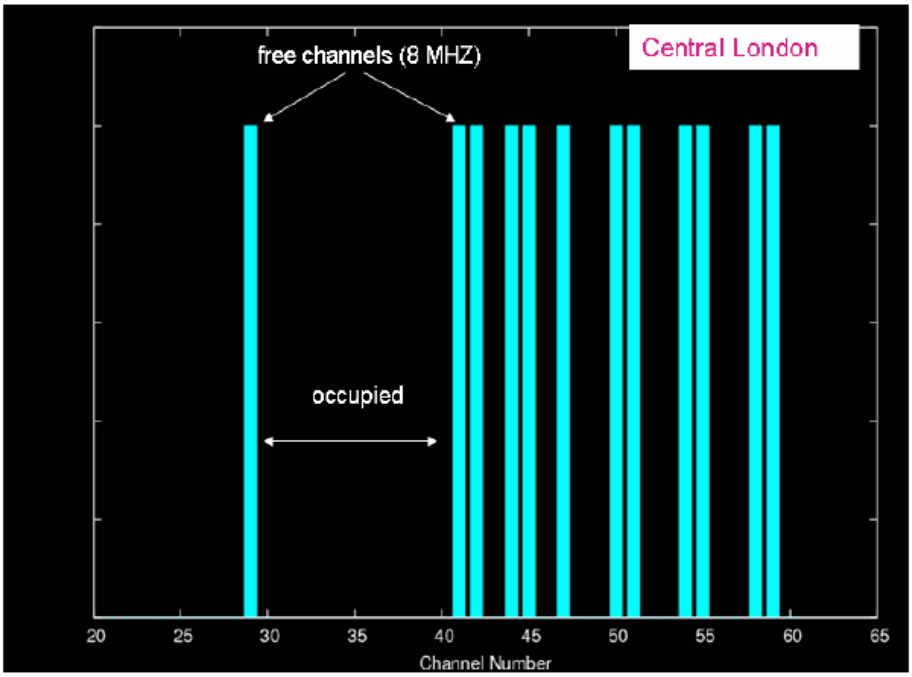

Figure 2: Contiguous TVWS Channels in Central London [3]

Figure 3 provides some examples of contiguous channel capacities for other UK locations.

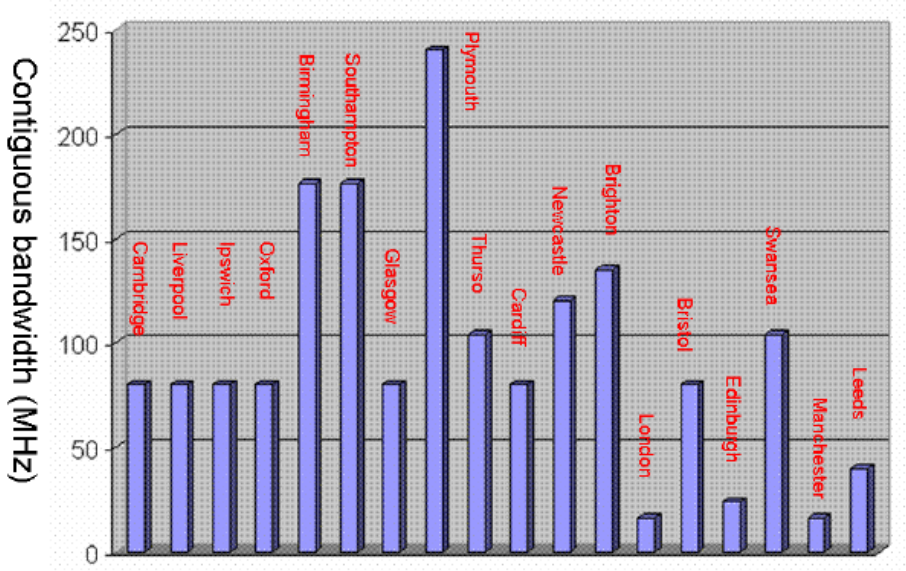

Figure 3: Maximum Contiguous capacity values for UK [3]

As evidenced in [18], the minimum number of TVWS channels available in the UK for a SU using a 10m antenna and transmitting at 15dBm, yielded an extra 80MHz of bandwidth for 90% of households and 184MHz for 50% of households, so confirming there are significant gains to be leveraged on available SU bandwidth within the TVWS band. The next section briefly reviews the regulatory steps to enable this unlicensed bandwidth to be exploited. It is interesting to note both Ofcom and FCC [18, 19] have opened a TVWS band for industry proposals, while recently the use of TVWS for autonomous vehicles has been proposed [20].

4. Regulatory Standards

The adopted Ofcom and FCC standards permit CRN broadband devices to operate in TVWS [12, 13, 21, 22], with the main TVWS engagement parameters specified by both regulators along- side the corresponding IEEE 802.22 standard [13, 15] values are defined in Table 1. These include: the respective probabilities of PU detection (P_d) and false detection (P_f), the DTT sensing noise floor, SU transmit RF power for a *base station* (BS) node in the presence of PU adjacent channels; and SU transmit RF power for a mobile node in the presence of PU adjacent channel.

Table 1: Regulatory TVWS engagement parameters [13, 15]

Rule	Parameter	OFCOM	FCC	IEEE802.22
1	DTT Sensing Threshold	-120dBm	-114dBm	-114dBm
2	Wireless Microphone Threshold	-126dBm	-114dBm	-114dBm
3	SU Transmit Power Fixed Network Node 1st Adjacent Ch - $P_{BS(N+1)}$	4dBm	16dBm	-
4	SU Transmit Power Fixed Network Node 2nd Adjacent Ch - $P_{BS(N+2)}$	17dBm	30dBm	36dBm
5	SU Transmit Power Mobile Network Node 1st Adjacent Ch - $P_{M(N+1)}$	4dBm	16dBm	-
6	SU Transmit Power Mobile Network Node 2nd Adjacent Ch - $P_{M(N+2)}$	17dBm	20dBm	-
7	Out-of-Band powers	<-46dBm	-55dBc	-
8	DTT Bandwidth	8MHz	6MHz	6MHz
9	Probability of Detection P_d	1	1	0.9
10	Probability of False Detection P_f	-	-	0.1

The Ofcom and FCC settings in Table 1 are committed to PU protection in their respective countries. Conversely, IEEE802.22 is a SU-focused standard, with the specified parameters being the maximum allowable transmit-power requirements, while corresponding PU protection is the responsibility of the respective country regulators. While sensing has been considered by the regulators, Ofcom currently has only proposed a geo-location database solution for industry consultation, while FCC is focusing on the database solution, with any sensing proposal having to undergo stringent certification with reduced radiating power [23].

The IEEE802.11af wireless networking standard [23], which is also known as White Space Wi-Fi (White-Fi) and Super Wi-Fi, permits WLAN operation in TVWS in both the VHF and UHF bands between 54 and 790MHz. CRN technology can transmit on unused DTT channels, with crucially this particular standard stipulating PU interference bounds.

5 Enabling Technologies for Spectral Sensing

Historically the *Open Systems Interconnection* (OSI) communication stack has been used to communicate information between layers, however for CRN applications this is limited by both parameter availability and acquisition time-scales. Once the parameters have been acquired, some analysis is required to interpret an unpredictable RF environment. In the regulatory parameter settings in Table 1, the RF transmit power can vary between a fixed SU BS and a mobile SU user. Furthermore, the mobile SU uses minimum RF power in order to minimise the local noise temperature outside the coverage area of the SU BS which can occur if the mobile SU is at the edge of the BS coverage area. To achieve the coverage area of a fixed SU BS, the mobile SU uplink must employ ad-hoc routing [24, 25]. The following sections detail some of the supporting technologies for CRN access of TVWS.

5.1 Cross Layer Processing

Cross layer processing (CLP) design strategies attempt to optimise key parameters by using information from other OSI layers, allied with information not readily available within the OSI communication stack. Unlike normal OSI stack information exchange, CLP is not constrained to information that is of necessity, contained within adjacent layers. This enables faster information retrieval because the information does not have to be transferred through several layers before reaching the requisite layer. Furthermore, not all information required within a layer to perform its function is passed to other layers, so CLP permits information to be utilised by any OSI layer.

The benefits of CLP are that it reduces the overhead within the protocol stack so lowering the time to acquire information and configure parameters. In [10], it was shown that if CR routing

in the network layer uses information from the spectrum management block then enhanced routing performance can be achieved.

There are two drawbacks of CLP. Firstly, proprietary information models must be implemented across the cross-layer block which will vary between implementations. Standards can be formulated between all stakeholders to frame a rigid information model for interoperability, however this requires considerable time overhead to establish such a standard. The second limitation is that a higher computational cost is incurred in implementing a CLP block with an associated increase in power resources.

To date, this has not been an issue in CRN research [10, 11], because the focus has largely been on the physical layer. Now however, the emphasis has shifted towards optimising resources to improve the *quality-of-service* (QoS) provision for the SU, so the CRN needs to simultaneously influence parameters in the significant OSI layers. Examples include optimising the RF power for routing to spectrum access decisions which are tailored to the application layer (Layer 7) requirements, which directly relate to the QoS user experience.

This chapter also introduces a novel cross-layer mechanism called the *cross layer cognitive engine* (CLCE) which shares information between the *medium access control* (MAC) and physical layers, so sensing measurements can readily influence spectrum access decisions. Some of the challenges in successfully implementing the CLCE [2, 15, 26] include:

- **Modularity** – The OSI layers are designed to be modular so they operate independently of each other. CLP design can compromise this property so avoiding technology-specific parameters being passed to the CLCE by abstraction alleviates the need for a bespoke solution in different cross-layer blocks.
- **Information Interpretability** – Choosing a knowledge representation base which is able to accommodate different implementations of the layer modules is vital.

- **Imprecision and Uncertainty –** Since parameters to be exported can contain measurement inaccuracies, cross-layer blocks must be able to manage imprecision which makes incorporating a fuzzy capability an attractive option**.**
- **Complexity and Scalability** - CRN must operate with different wireless configurations to be able to be scalable, so to optimise the wireless link to user requirements, the cross-layer block can become complex because of the number of possible parameters to be exported.

A number of cross-layer block implementations currently exist, with the most prominent being considered below [26, 27, 28, 29]:

- **Radio Knowledge Representation Language** [28, 29] - Each micro-world represents a specific wireless technology which implies the CLCE needs explicit knowledge about these technologies. This is contrary to the aforementioned modularity and scalability features.
- **Artificial Intelligence (AI)** [2, 27, 30] - Solutions such as neural networks and genetic algorithms are well suited to handling large datasets, but they concomitantly require long training periods to be effective which is not practical in most wireless applications.
- **Fuzzy Logic Controllers** [2, 26, 27] – These are modular, so technology-specific information is retained in the layers with more generic information used in the cross-layer block. Improved information interpretability is achieved using linguistic attributes for each defined membership function. Precision and accuracy issues are avoided by using an imprecise knowledge representation base. The complexity of the cross-layer block is also lower than other proposals.

5.2 Ad Hoc Routing

Section 4 stressed that regulatory requirements mean the RF transmit power of both fixed and mobile SU nodes can vary up to the maximum values in Table 1, and because of the fixed node antenna height being higher than the mobile node, greater coverage is achieved. To compensate for this asymmetrical coverage in the down and uplink directions, ad hoc routing can be innovatively applied in the uplink direction (mobile to fixed node) to achieve the same coverage in both directions.

To enable frequency re-use and thus increase spectral efficiency, low RF power needs to be used, though a corollary of this is that ad-hoc routing must be employed to ensure CR messages reach their destination via other CR nodes. To minimise latency in time sensitive applications consideration must be paid to how the message is routed through the CRN to their destination [2, 15).

Routing protocols for *mobile ad-hoc networks* (MANET) [2, 15, 24, 25] are well established, though CRN introduce some new challenges which need to be solved. These include:

i. Link Availability - In the example in Figure 4, there is a short spectral hole for the CRN to exploit, however unlike in a MANET, the availability window is measured in milliseconds rather than seconds, except in the case of TVWS.

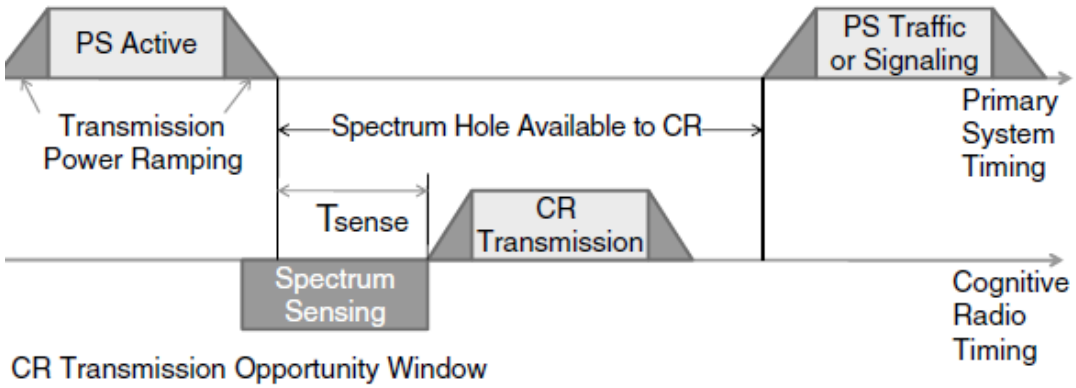

Figure 4: CRN Transmission Opportunity Window [15]

ii. Unidirectional links – Typical wireless networks use bi-directional links though this is questionable for CRN for the above reason. Also, in TVWS scenarios, due to the regulatory SU unidirectional power allocation, pragmatically there is only the prospect of uni-directional links which imposes a specific design constraint on the network layer.

iii. Heterogeneous wireless networks – Normal wireless networks are structured while CRN have a more ad-hoc, heterogeneous node structure. This means CRN require inter-system handover, but with very short duration links routing relying on cooperative relaying. Such heterogeneous networks pose a security risk because the link duration is so small, there is insufficient time to authenticate any security certificate.

Reactive protocols devised for typical wireless networks can be adopted for CRN to overcome some of the above issues. The two most common routing protocols are *Dynamic Source Routing* (DSR) [24] and *Ad-Hoc On Demand Distance Vector* (AODV) [25].

The DSR protocol is based on source routing whereby all the routing information is maintained by the mobile nodes. It is a simple and efficient routing protocol designed specifically for use in multi-hop links for mobile nodes. DSR allows the network to be completely self-organizing, without the need for any existing network administration. The protocol is composed of two main phases namely "Route Discovery" and “Route Maintenance", which work together to allow nodes to discover and maintain routes to destinations in the ad hoc network. All aspects of the protocol operate entirely on demand, allowing the routing packet overhead of DSR to scale automatically, since only after a route to the destination node has been identified does packet transmission occur.

In contrast, the AODV routing protocol is intended solely for use by mobile nodes in ad hoc networks. It offers quick adaptation to dynamic link conditions, low processing and memory overheads, low network utilization, and determines unicast routes to destinations within the

network. AODV route table entries are dynamically setup at each intermediate node as the packet is transmitted towards the destination so reducing the traffic overhead.

6 Existing Sensing Techniques

The regulatory framework in Table 1 has formed the basis for a variety of spectrum sensing proposals including non-cooperative feature sensing and cooperative sensing using a non-Gaussian noise covariance Rao test. This section critically analyses these sensing solutions within a regulatory context.

6.1 Non-cooperative feature sensing

In [21, 22], an autocorrelation algorithm for spectrum sensing was developed based upon the correlation of the frame headers and synchronisation blocks which are a form of matched filter feature detection. Spectrum sensing is explored in the context of the three main TV standards deployed in China, namely Digital Terrestrial Multimedia Broadcast (DTMB), China Multimedia Mobile Broadcasting (CMMB) and Phase Alternating Line –D/K (PAL-D/K). For comparative purposes, only DTMB is considered in this discussion because it is the standard that most closely resembles the UK DVB-T standard in term of frame structure and transmission bandwidth. In [21], a simulation platform was constructed along with a prototype model with the detection results being displayed in Figure 5.

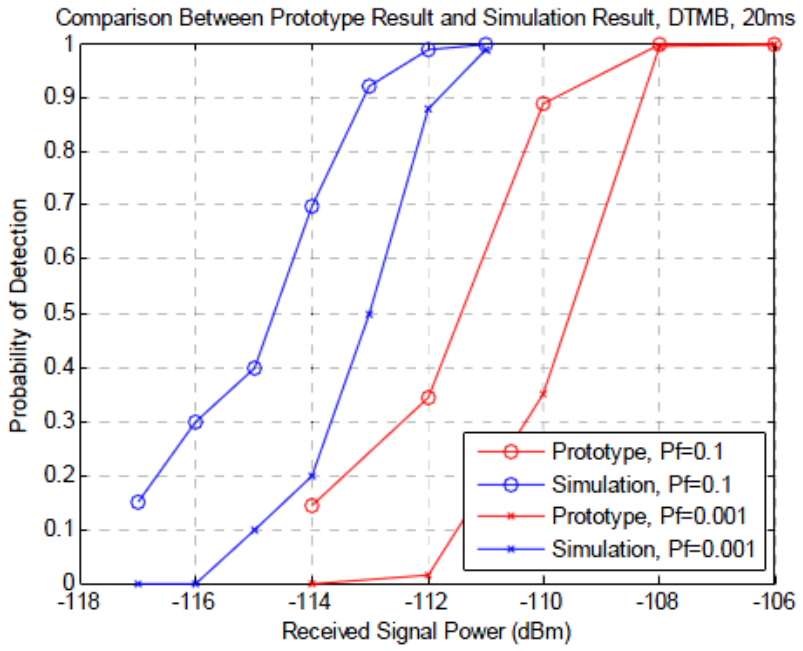

Figure 5: Simulation and laboratory results for DTMB detection [21]

Figure 5 shows both the simulation and laboratory prototypes at *false detection rates*, $P_f = 0.1$ and $P_f = 0.001$. The *detection rate* (P_d) for the prototype is generally 3 to 4 dB lower compared to the simulation results which is explained by the simulation not including analogue RF stage impairments like frequency offsets and amplifier nonlinearity. Interestingly, by comparing the detection and false detection probabilities for the IEEE 802.22 standard, $P_d = 0.9$, $P_f = 0.1$ at a signal strength of -114dBm (Table 1), while the corresponding simulation results for $P_f = 0.1$ in Figure 5 reveal only a $P_d = 0.7$ at -114dBm, so this sensing solution fails to comply with the IEEE 802.22, Ofcom or FCC requirements defined in Table 1.

The North American approach [22] examined the development of spectrum sensing algorithms for *Advanced Television Systems Committee* (ATSC), *National Television System Committee* (NTSC) and radio microphones. Sensing for both ATSC and NTSC involves a unified signature-based, spectrum sensing algorithm, which in the case of the US DTT standard ATSC, is the autocorrelation of the SYNC segment of the frame.

ATSC results are plotted in Figure 5, which shows detection probability (P_d) against the probability of false detection P_f at different SNR values.

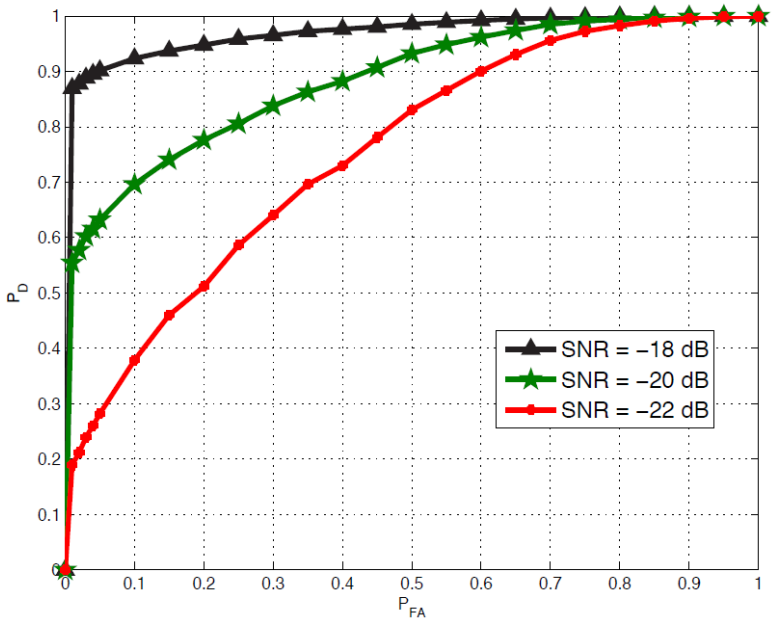

Figure 5: Probability curves for ATSC DTT Signals at different levels of SNR [22]

If a noise floor of -100dBm is assumed within a 6MHz bandwidth, which is the TVWS bandwidth in USA, then a SNR = -18dB is represented by a signal of -118dBm which is below the sensing threshold of -114dBm for both IEEE 802.22 and FCC (Table 1). From Figure 5, at SNR = -18dB, P_d =0.9 and P_f = 0.05 which is the only SNR value which upholds IEEE 802.22, though it still does not comply with the FCC detection probability requirement in Table 1. The other SNR values (-20dB and -22dB) do not comply with IEEE 802.22 and FCC sensing thresholds.

6.2 Cooperative sensing using a non-Gaussian noise covariance test Rao [31]

Spectrum sensing for CRN in the presence of non-Gaussian noise is challenging due the CR having to have knowledge of both the PU and SU. To overcome this limitation, the *generalized likelihood ratio test* (GLRT) can be applied which combines unknown parameter estimation with a likelihood ratio test. While GLRT is an optimal detector, it must compute a maximum

likelihood estimation (MLE) for the received signal power of the desired signal, the noise variance and the unwanted signal and so consequently incurs a large computational burden. The Rao test is an approximate form of the GLRT which only estimates system model parameters for unwanted signal conditions. This simplifies the Rao structure and [31] examined it's use in the cooperative mode, which is a commonly used technique in spectrum sensing since it overcomes the harmful effects of fading and shadowing by taking advantage of spatial diversity. It thus offers a solution to PU sensing for non-Gaussian noise conditions. Cooperative spectrum sensing is a viable solution for a CR sub-network comprising one SU BS and multiple SU mobiles, which collectively detect the presence/absence of a PU within a given frequency band. Each SU employs a Rao detector to independently sense the PU signal in the presence of non-Gaussian noise, with local SU decisions then forwarded to the BS which makes a final access decision.

The co-operative spectrum sensing system in [31], is an IEEE 802.22-based solution that uses the Rao test to measure the non-Gaussian noise level to improve the energy detection performance and includes a multi-user extension where β defines the noise model used. Figure 6 shows the results for four SU sensors at differing β settings which represent various noise profiles ranging from Gaussian (β=2) to Laplacian (β=1). Also, the results evaluate four strategies for cooperative sensing. The first is the traditional cooperative sensing technologies (OR, AND) where the proposed solution uses the cooperative technologies coupled with the Rao test measure.

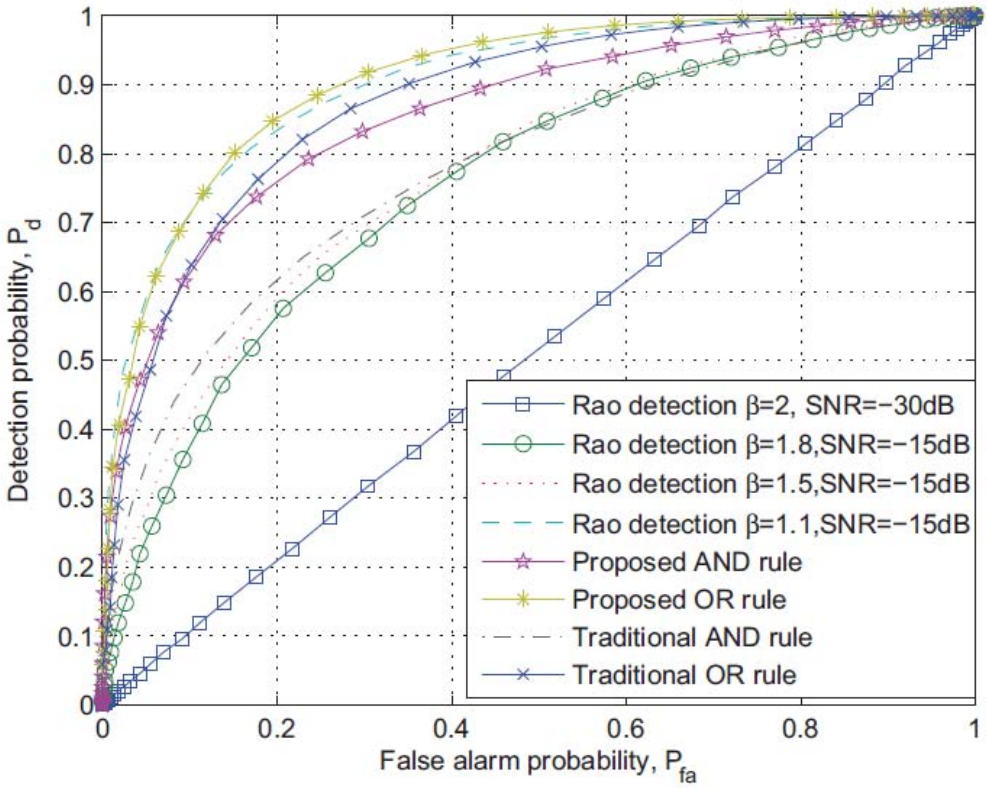

Figure 6: Family of ROC curves of cooperative for different values of β [31]

In summarising, the results for both non-cooperative sensing in [21, 22] and cooperative sensing [31] corroborate that the requisite detection and false detection rates specified in Table 1 are not upheld. This provided the motivation to investigate new sensing strategies which are able to fulfil the strict sensing regulatory requirements of OFCOM and FCC, with one innovative solution being detailed in the following sections.

7. ENHANCED DETECTION ALGORITHM (EDA)

This PU detection technique [17, 32, 33] was introduced to specifically facilitate access to TVWS channels by employing the *cross-layer cognitive engine* mechanism introduced in Section 5.1. This shares information between the MAC and physical layers, so energy sensing measurements can dynamically influence the DSA decisions [10, 17]. EDA exploits inherent

patterns in the DTT frequency deployment to determine whether a PU occupies a particular DTT channel using a fuzzy logic model to make channel occupancy decisions. By scanning adjacent frequencies on either side of the channel under investigation, this effectively turns the energy detector into a feature detector, with a *scan range* parameter *B* determining the number of channels to be sequentially scanned. Hence, if *Ch_A* is the DTT channel under review, EDA symmetrically scans *Ch_A*±1, *Ch_A*±2… up to *Ch_A*±*B*. Symmetrical scanning is used due to the equi-probability of a neighbouring DTT channel being either below or above the channel of interest.

EDA affords a unique sensing option for DTT transmitters because regional DTT frequencies are deployed in clusters of 6 channels in the UK and due to DTT domestic receiver antennae groupings [34], these 6 channels can only lie within a possible bandwidth of 16 DTT channels. The corollary is that by scanning *B* channels either side of the channel of interest, the majority of occupied DTT channels in a region are detected, with crucially, low false detection probabilities being achieved by maintaining a low *B* value. Selecting the best choice of *B* will be discussed shortly. EDA uses the sensed energy values in the scanned channels to resolve whether the DTT channel is occupied. This approach allied together with a geo-location database means EDA generates an accurate map of PU channel usage. The advantage of EDA, when coupled with a geo-location database, is that an accurate mapping of PU channel usage is obtained. PMSE devices can also be included in the database so reducing PU interference and increasing the available bandwidth for SU.

The next section introduces the design principles underpinning EDA.

7.1 EDA Design

Figure 7 shows a block diagram of the EDA [17, 32, 33], with fuzzy logic inference model employing a classical fuzzy logic framework [26], so I/P (input) A is the sensor output for the channel under investigation, while I/P B is the maximum sensor output for 1 to *B* channels either up or down from the channel under investigation.

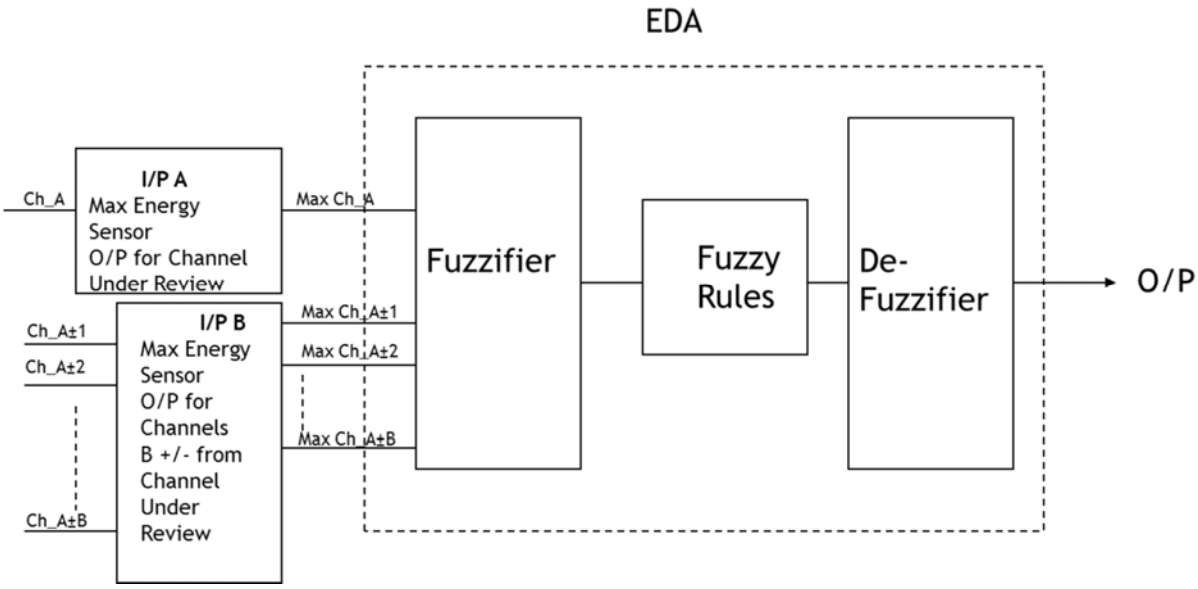

Figure 7: EDA Block Diagram [17, 32, 34]

The role of the fuzzifier is to translate the input into a fuzzy set which is allocated a membership function. This follows a normal (Gaussian) probability function used for RF detection. The fuzzy rule block defines how EDA behaves under practical conditions, while the de-fuzzifier produces a final crisp output using the *centre of area* method [26].

7.2 *B* Parameter Selection

The choice of *B* is critical to EDA detection performance as it scans channels up and down from the channel under investigation to *B*, where *B* is the integer number of channels to be scanned. Three membership functions *Lo*, *Med* and *Hi* are used to assess the occupancy status of a specific channel. If a particular channel lies within the *Med* probability range and another channel which is either within *B* up or down and also lies within either the *Med* or *Hi* probability detection ranges, then the outcome is weighted according to a set of fuzzy rules [34] which is defined above and a crisp occupied or unoccupied result is returned. This reflects the phenomena that DTT channels in a local area are generally deployed in a cluster configuration

due to DTT antenna groupings [34] in which another DTT channel either *B* channels up or down can be located. EDA detection/false detection response against *B* for signal strength of -120dBm and averaged over 22 Major DTT transmitter sites in the UK, is shown in Figure 8, with *B* dynamically determined. Note, *B* will always be bespoke to the country of the DTT channel deployment.

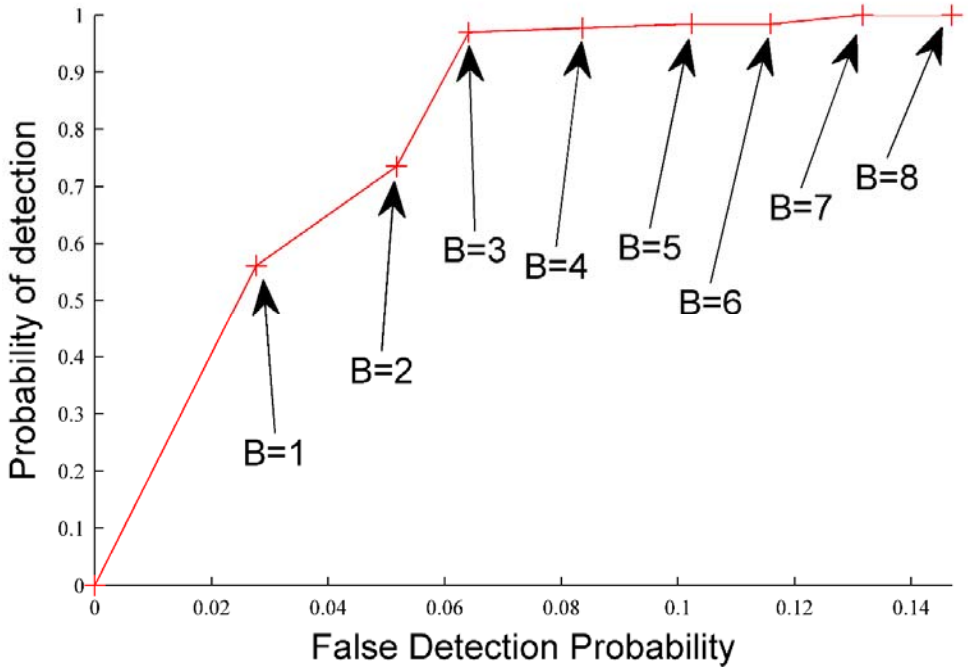

Figure 8: *B* Response for the UK

The corollary from Figure 8 is that by scanning *B* channels either side of a channel of interest, the majority of occupied DTT channels in a region are detected with crucially, low false detection probabilities P_f achieved by maintaining a low *B* value. EDA then uses the sensed energy values in the scanned channels to determine whether the DTT channel is occupied.

7.3 EDA Performance

The detection performance of EDA is shown in Figure 9 in comparison with [21]. This reveals EDA consistently out performs existing PU detection algorithm by up to 9 dB when applying

the IEEE 802.22 standard detection thresholds of P_d = 0.9 and P_f = 0.1, though importantly both techniques fail the stringent Ofcom requirement of P_d = 1.0 at a signal strength of -120dBm.

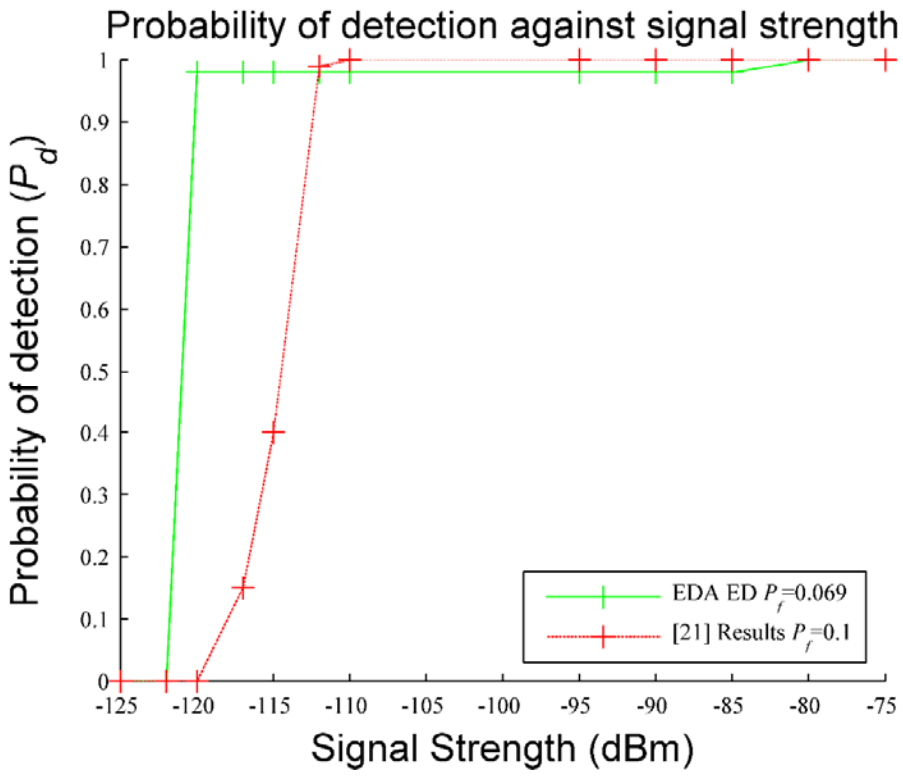

Figure 9: Detection Probabilities versus Signal Strength

Despite its performance limitations, EDA demonstrated that a sensing strategy for TVWS applications was feasible and consequently it became an integral constituent block in a novel adaptive-based sensing framework known as *Generalised EDA* (GEDA) [17], which achieves 100% PU detection under for all regulatory scenarios. GEDA will now be reviewed.

8. GENERALISED EDA (GEDA)

8.1 Introduction

As highlighted in Section 7, while EDA upholds the P_f=0.1 requirement of IEEE 802.22 [22], it failed to achieve P_d =1.0 for the DTT sensing threshold in Table 1. This provided the motivation for the development of the GEDA paradigm, which reuses key EDA components,

while crucially integrating a new adaptive mechanism for selecting the B parameter to secure significant performance improvements.

8.2 GEDA Design

Figure 10 shows the block diagram of the GEDA model which reveals the key role EDA plays. In comparison to EDA, GEDA introduces three new system parameters, namely B_{Pri}, B_{Sec} and a *scaling factor* (*SF*). B_{Pri} is the initial scan range value of B used to evaluate channel occupancy in accordance with the IEEE 802.22 standard i.e., $P_d = 0.9$ and $P_f = 0.1$, while B_{Sec} is a higher B value, if required, which ensures an overall $P_d = 1$ once the first frequency scan using B_{Pri} has been completed. It is important to stress that B_{Sec} cannot be directly used at the outset of sensing by GEDA because its higher value increases the likelihood of false detections which compromises detection performance. It is thus, only used on occupied DTT channels that B_{Pri} cannot detect. Both B_{Pri} and B_{Sec} are country-specific and are determined applying EDA using the corresponding B value that yields the respective P_d and P_f values.

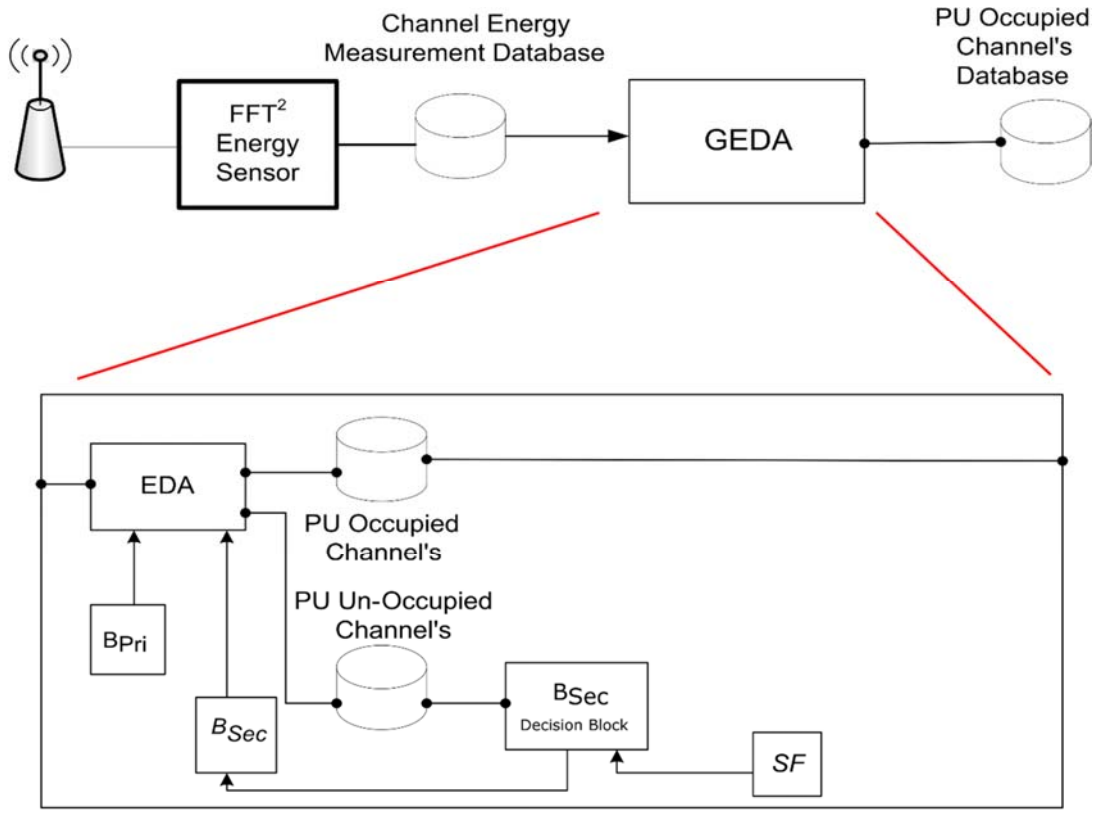

Figure 10: GEDA Block Diagram

GEDA detection can thus use either B_{Pri} or B_{Sec} for its DTT scanning range. The former is the initial scan range B value, and, in many cases, this is the only value required. In a few cases however, B_{Sec} has to be used to achieve P_d =1. Whether B_{Sec} is used is governed by the *SF*, which is the ratio of the highest to the lowest DTT frequency energy values, both of which are stipulated by the relevant regulatory authority [13, 34]. The role of *SF* will now be further investigated.

8.2.1 Scaling Factor (SF)

Using this highest frequency (lowest RF energy) to the lowest frequency (highest RF energy) ratio enables a window of energy measurements to be defined within which it is feasible that a PU DTT channel may trigger using B_{Sec}, provided the channel is in the unoccupied channel

database. Thus, by scaling the lowest frequency energy measurement in the DTT channel occupied database obtained using B_{Pri}, a threshold for using B_{Sec} on an unoccupied DTT channel is established. *SF* is formally expressed as:

$$SF = \frac{\left|\mathcal{F}\left(RSS_{Hi\_DTTFreq}\right)\right|^2}{\left|\mathcal{F}\left(RSS_{Lo\_DTTFreq}\right)\right|^2} \quad (1)$$

where $RSS_{Hi\_DTTFreq}$ and $RSS_{Lo\_DTTFreq}$ are the respective *received signal strength* (RSS) measurements for the highest and lowest DTT frequencies for a preset distance between the DTT transmitter and receiver.

8.2.2 GEDA Mechanism

Using B_{Pri}, the initial PU sensing results are determined using EDA, from which a PU unoccupied list is compiled. If the criteria in equation (2) is upheld, EDA is reapplied but this time the DTT channel scanning is performed using B_{Sec} to assemble the final PU DTT channel occupied list [17] with *y* being the energy measurement of the lowest occupied DTT channel.

$$IF\ unoccupied\ DTT\ channel\ energy\ \geq y \cdot SF \quad THEN\ B = B_{Sec} \quad (2)$$

8.3 Numerical Evaluation of the GEDA mechanism

To demonstrate how GEDA resolves undetected PU channels which are outside the B_{Pri} capture range, we shall examine the Yorkshire Belmont UK scenario. To illustrate how GEDA is easily transferrable to other countries, the Washington DC FCC (6) scenario is also examined.

8.3.1 Yorkshire Belmont - UK Channel Deployment GEDA analysis

The first part of the analysis is where the B_{Pri} value is calculated for the UK DTT channel deployment plan using the algorithm in Section 8.2. From this analysis, B_{Pri} = 4 which gives a P_d of 0.98 and P_f of 0.0692.

From this DTT channel deployment, the B_{Sec} parameter will be invoked for two transmitter sites, namely Yorkshire Belmont and Central-Waltham. For the latter case, only one channel is not detected by B_{Pri} however, using B_{Sec} in the same transmitter region resolves this channel. Yorkshire Belmont is chosen as the most challenging case study due to having two PU channels not detected while Scunthorpe is the location for the SU BS, since it is at the edge of the DTT transmission area. The two channels which are not resolved to be occupied are DTT channels 53 and 60, and the way GEDA effectively resolves these channels for the Yorkshire Belmont DTT transmitter is detailed in [5] and is summarised here.

Firstly, the *SF* for the UK is calculated from (1). The lowest DTT frequency in the UK is 474 MHz and the highest is 786 MHz and the energy references were 60Km away from a 100KW DTT transmitter. The DTT propagation model is used to obtain the two energy values below from the sensor with stated parameters:

$$SF = \quad 3.4482118 \times 10^4 / 1.4930635 \times 10^5 = 0.23$$

The next step is to map the Yorkshire-Belmont scenario which is shown in Figure 11, where Yorkshire Belmont is the primary DTT transmitter, and Saddleworth, Sheffield and Waltham are respectively the adjacent region transmitters.

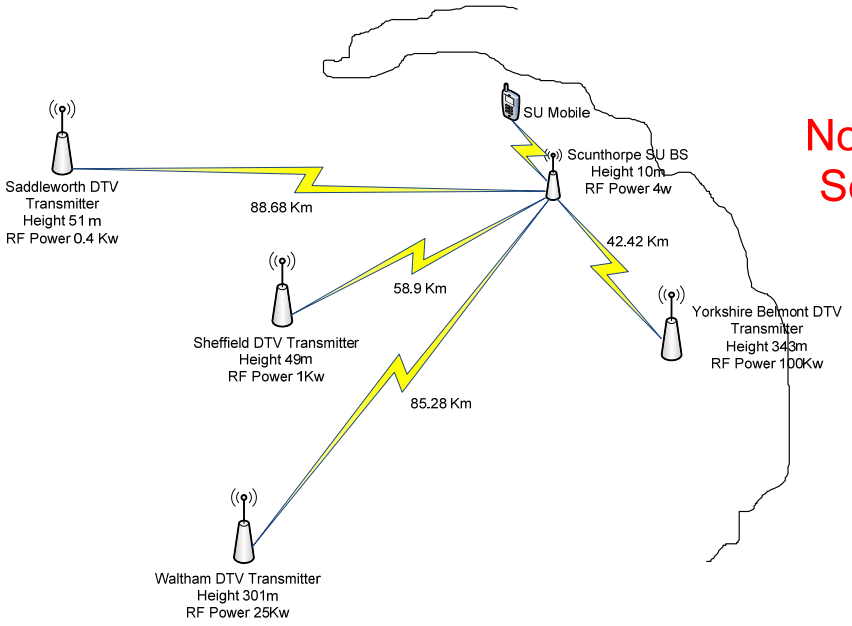

Figure 11: Yorkshire Belmont Analysis

The energy responses for each DTT transmitter is calculated to a SU BS in Scunthorpe by the DTT distance model using the SU BS antenna height (10m). The corresponding sensor results are shown in Table 2.

Table 2: Energy responses for the Yorkshire Belmont transmitter area to a Scunthorpe SU BS

Transmitter Site and Channel	Sensor Measurement at SU BS in Scunthorpe
Saddleworth Ch 39	6.0904529×10^{1}
Sheffield Ch 21	6.2628017×10^{1}
Waltham Ch 29	6.3129225×10^{1}
Yorkshire Belmont Ch 53	2.5336327×10^{5}
Yorkshire Belmont Ch 60	2.0449943×10^{5}

Yorkshire Belmont Ch 22 lowest Channel detected by GEDA using B_{Pri}	8.4410224×10^5

The next step is to calculate the trigger for expediting a scan for a channel using B_{Sec}. This is calculated from taking the lowest frequency channel sensor measurement which is detected by the GEDA using B_{Pri} which in this case is channel 22 and multiplying by *SF* (0.23) to obtain the trigger point. From Table 2, this will be $8.4410224 \times 10^5 \times 0.23 = 1.94143 \times 10^5$.

Now applying GEDA, the unoccupied channel scan using B_{Sec}=7 is conducted and if the channel sensor output is $\geq 1.94143 \times 10^5$, which means from Table 2, the Yorkshire Belmont DTT channels 53 and 60, then the B_{Sec} parameter is triggered. This means when applying B_{Sec} = 7 both these DTT channels are detected.

The GEDA mechanism has been fully validated for all UK scenarios though not all countries follow the same channel deployment rules. Hence in order to demonstrate the agility of this novel sensing algorithm, an alternative North American scenario is now presented to exhibit this flexibility.

8.3.2 Washington DC - North American Channel Deployment GEDA numerical analysis

The major differences between the North American and UK scenarios are:

1. The DTT channel bandwidth utilised in North America is 6MHz as opposed to 8MHz in the UK.
2. The modulation scheme utilised in North America is 8 *Vestigial Sideband* (VSB) modulation where in the UK both 64 and 256 *Quadrature Amplitude Modulation* (QAM) are used.

3. The way the DTT channels are distributed is quite different and mainly driven by geography. In the North American case, distributed transmitter sites [6] are used to service a region because real estate is not a driving factor, with the number of channels varying between 3 to 21 depending on terrain and size of region.

For this analysis, data is required upon channel and RF parameters for the DTT deployment which is generally available from the relevant regulator (6). Using the channel deployment in [6], P_d was calculated using $B_{Pri} = 4$ giving a $P_d = 0.9016$ and $P_f = 0.053$, which conforms to the IEEE 802.22 P_d and P_f criteria. The channel deployment matrix is converted into a detection matrix by using the previously mentioned *detection probability* algorithm.

From the detection matrix, it was noted that channel 15 for Washington DC was not detected when using $B_{Pri} = 4$. Figure 12 shows the Washington DC DTT transmitter model along with a SU BS in the centre of Washington in which this forms the basis of the analysis, with 10 DTT channels allocated to the Washington DC region, supported by 6 transmitter sites. Each transmitter is identified by a four-letter call sign, with the particular transmitter of interest being WFDC, which is the channel which cannot be detected. WNVC is the transmitter whose channel is the lowest frequency detected using B_{Pri} while WMPB is in the adjacent region to Washington DC.

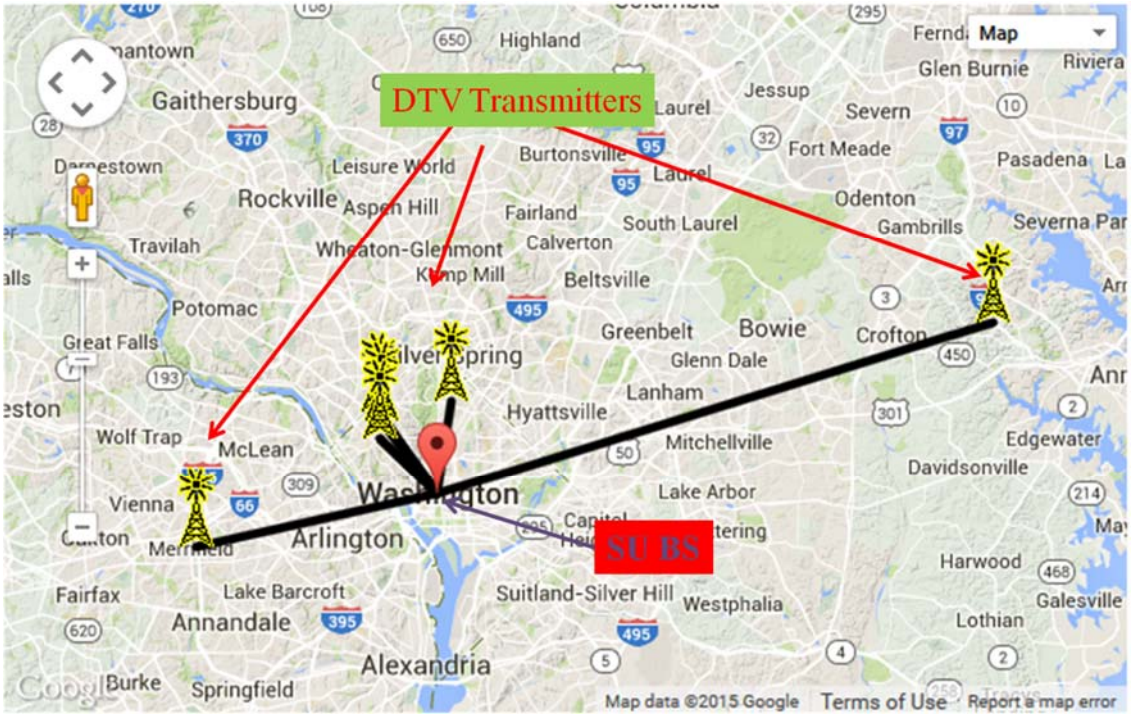

Figure 12: Washington DC DTT Model [6]

Channel 15 cannot be detected using B_{Pri} and the lowest frequency which can be detected using B_{Pri} is channel 24. Figure 13 shows the model for these two transmitters WNVC (Channel 24) and WFDC (Channel 15). WMPB (Channel 29), which is a channel servicing Baltimore which is an adjacent region to Washington DC, is also included to demonstrate that false triggering of B_{Sec} will not be caused by any adjacent region, as this would have the effect of increasing the probability P_f, thereby unnecessarily triggering B_{Sec}.

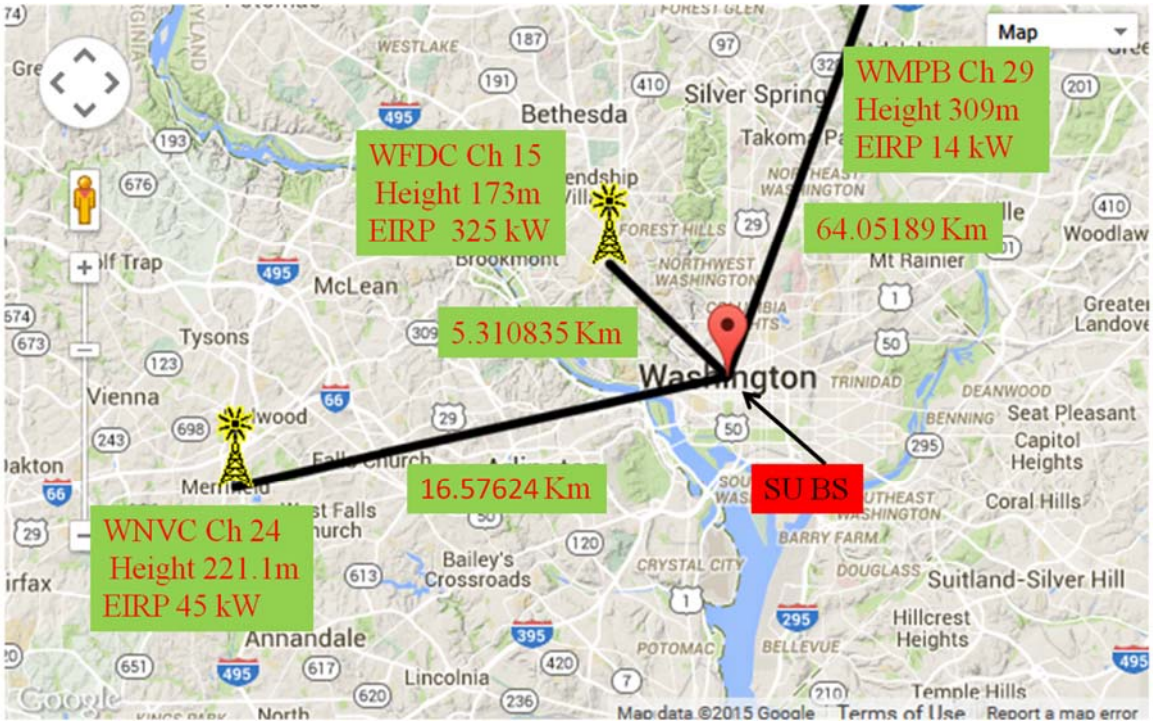

Figure 13: Washington DC - WNVC, WFDC and WMPB DTT Model [6]

WFDC (channel 15) is not detected using B_{Pri} and WNVC, which is the lowest frequency detected in the Washington DC region thus defines the value at which B_{Sec} is to be used in conjunction with *SF*. Again using (1), the *SF* is calculated using the lowest and highest DTT frequencies in the US, which are 473 MHz and 887 MHz respectively.

$$SF = \quad 1360281 / 7907096.5 = 0.172033$$

This value is now used to calculate the sensor outputs for the three transmitters in Figure 13 to the SU BS in Table 3.

Table 3: Washington Model sensor measurements

Transmitter Site and Channel	Sensor Measurement at SU BS in Washington
WFDC Ch 15	1.1846454×10^{10}

WMPB Ch 29 Adjacent Region	4.9109495×10^4
WNVC Ch 24 lowest Channel detected by GEDA using B_{Pri}	2.0910753×10^7

As with the UK scenario, the next step is to determine the trigger for advancing the scan for a channel using B_{Sec}. This is calculated by taking the lowest frequency sensor measurement detected by GEDA using B_{Pri}, which in this case is channel 24 and multiplying it by SF (0.172033) to give the trigger point. Using Table 3, this is $2.0910753 \times 10^7 \times 0.172033 = 3.597339 \times 10^6$. Now applying GEDA, the unoccupied channel scan using B_{Sec} is conducted and if the channel sensor measurement is $\geq 3.597339 \times 10^6$ then this means for WFDC (channel 15) B_{Sec} is triggered. Thus, by using $B_{Sec} = 9$ in both the detection and false detection algorithms, this channel is successfully detected.

8.4 GEDA Results

The sensing performance of GEDA has been critically compared with two disparate DTT datasets. The first is DTMB which is the DTT standard in China (21), while the other is a North American study [22]. Both results were generated from a DTT deployment matrix of 22 sites. Given the Chinese scenario closely follows the UK in terms of DTT bandwidth and modulation schemes, this was compared to GEDA in a UK scenario using the same channel bandwidths and modulation schemes.

8.4.1 UK GEDA Results compared to DTMB Standard [21]

DTMB channels have a bandwidth of 8 MHz and employ 5 modulation constellations, namely 4-QAM NR, 4-QAM, 16-QAM, 32-QAM and 64-QAM. The UK DTT standard DVB-T also

has 8 MHz channels but only two modulation constellations, which are 64-QAM and 256-QAM. To ensure the worst case UK scenario is evaluated for GEDA, the latter is used because 64 QAM will display a greater energy level than 256 QAM i.e. higher signal bit energy per noise energy (E_b/N_o) is required to decode 256 QAM signals for the same throughput as per Shannon's Law [35].

The B_{Pri} and B_{Sec} values are calculated using the detection and false detection probability algorithms for compliance to P_d =1 and found to be B_{Pri} = 4 and B_{Sec} = 7 for the UK scenario. The GEDA results are displayed in Figure 14 along with the corresponding Chinese detection rates [21] at a P_f =0.1. The results confirm that unlike DTMB, GEDA achieves P_d =1 at a signal strength of -120dBm in accordance with Ofcom requirements (Table 1) and overall produces a 9dB improvement over [21]. It also achieves a lower comparative P_{fd} =0.069 compared to 0.1 in [24].

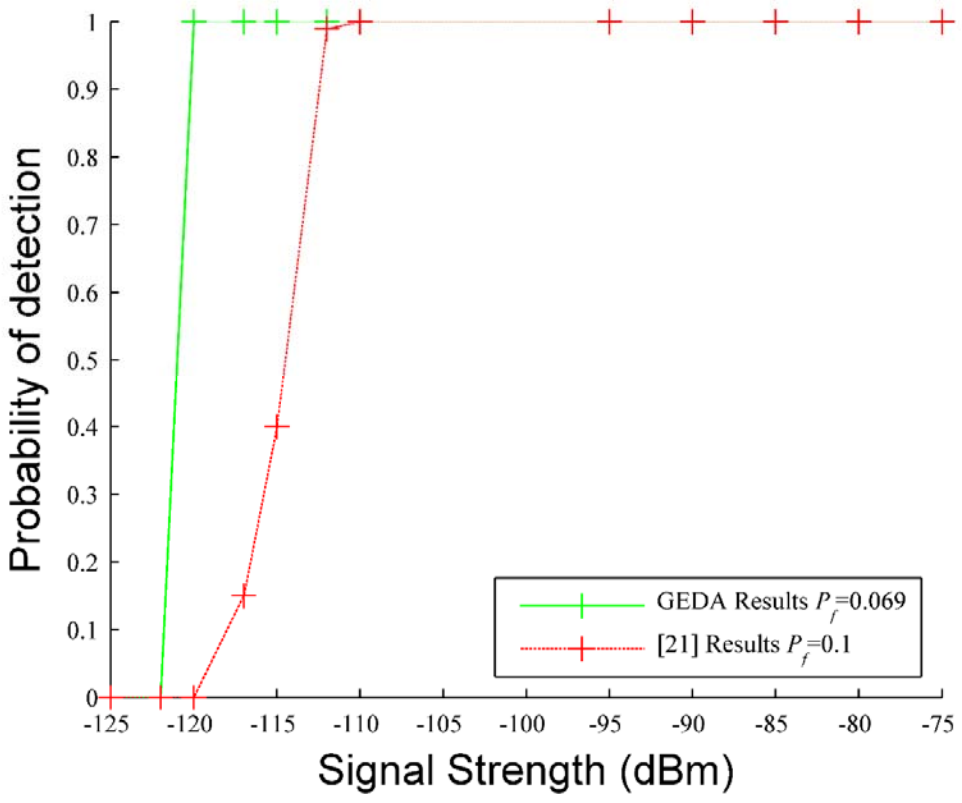

Figure 14: Comparative detection results for GEDA and DTMB standard

8.4.2 US GEDA Results

The next set of results in Figure 15 show how GEDA performs against the associated North American scenario in [22]. For FCC channel deployment, B_{Pri}=4 and B_{Sec}= 9, however to have an equitable comparison, both B_{Pri} and B_{Sec} values were varied between 1 and 9 so a wide range of P_f values were analysed.

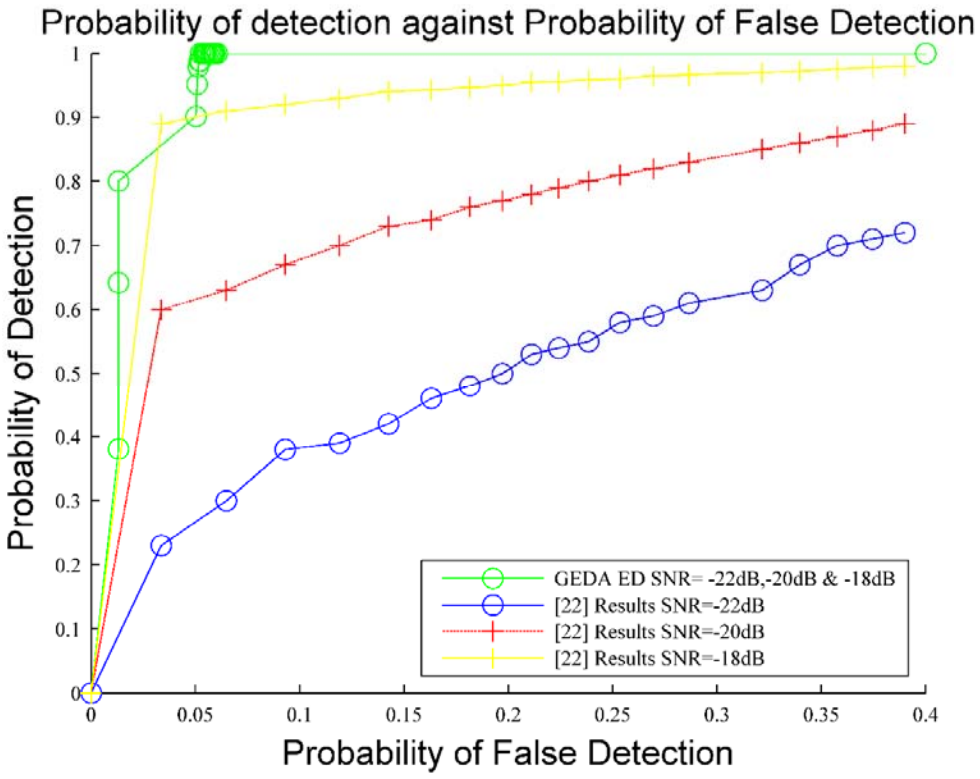

Figure 15: FCC SNR GEDA Results

The results clearly demonstrate GEDA superior robustness across the range of SNR values. The reason for this is that the comparators in [21] and [22] depend on the detection of frame

headers, which requires a certain SNR to exist. In contrast, GEDA energy measurements are combined with DTT channel deployment patterns, which effectively becomes a feature detector that is not dependent on demodulating the frame and is thus autonomous of the prevailing noise environment.

8.4.3 Comparison of GEDA results for UK and US

In Figures 14 and 15, GEDA has been evaluated against other sensing solutions deployed in the UK and US, however GEDA was not compared using the same criteria. This section analyses GEDA performance for both countries using SNR, and the detection and false detection metrics, with Figure 16 displaying their comparative performance.

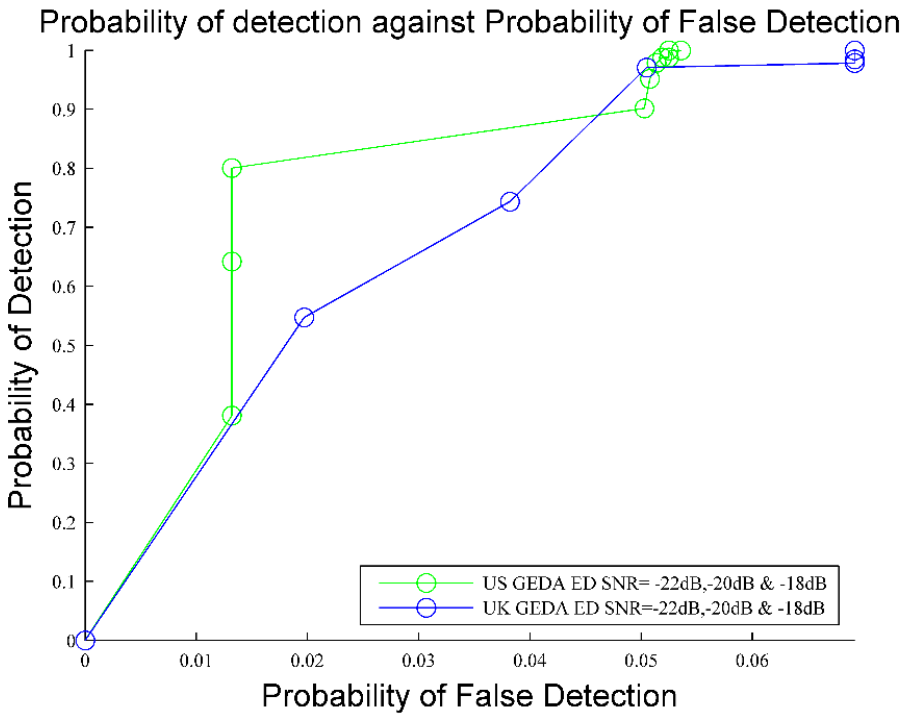

Figure 16: Comparison between GEDA UK and US results

The graphs show the US sensing results attain a P_d = 1 before GEDA, though both sets of results secure a P_d = 1 and P_f = 0.1 to uphold both regulatory and IEEE 802.22 requirements.

The difference is attributable to the diverse DTT channel deployment patterns between the UK and US (demonstrated by different the *B* values used) for the same sensing threshold = -120dBm.

9. Bandwidth available for TVWS devices

This section critically evaluates the potential of TVWS to make available extra bandwidth for SU cognitive devices. Two key concepts are firstly introduced.

i) The *Protection Contour* [34], which is a function of the DTT receiver being able to decode a DTT picture signal, even at the edge of a reception area, without incurring co-channel interference.
ii) The *Keep Out Contour* which combines the protection contour and hidden node issue to establish a dedicated sterilisation zone for each specific DTT channel.

To consider how real DTT systems operate in the UK, both the average coverage distance from the transmitter for the Mendip area [17, 34], and the matching Egli terrain factor were calculated. Using the Mendip DTT area as the case study [34], without loss of generality, the Egli terrain value was empirically found to be 97%. It will now be shown how the concepts of a *Protection Contour* and *Keep Out Contour* can be innovatively coupled to define how much bandwidth is available for SU TVWS cognitive devices to access. Each will be now individually considered.

9.1 Protection Contour and Interference Management

This contour [34] crucially depends upon the RSS at the edge of the Mendip DTT area, which is the worst-case scenario for a PU where no co-channel interference occurs. The related protection contour geometry is shown in Figure 17.

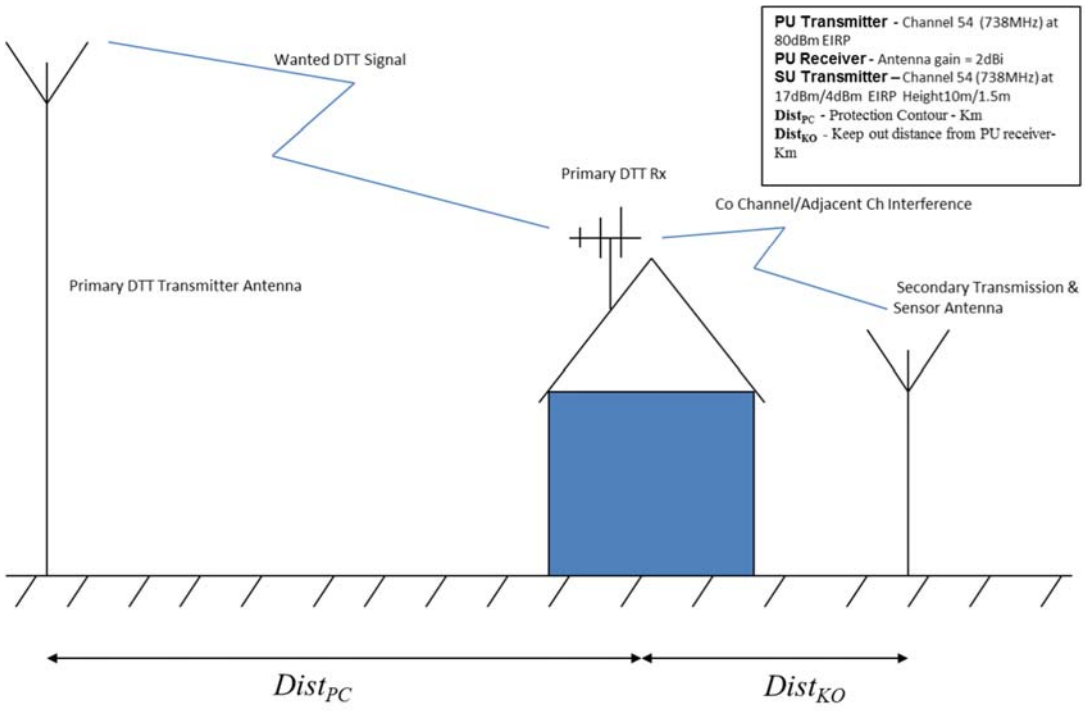

Figure 17: Protection Contour Geometry for the Mendip DTT area

The *protection contour distance* (*Dist*$_{PC}$) [34] at the edge of the receivable DTT signal (BER=*2*x*10*$^{-6}$) for the Mendip area is 54.023 Km for Channel 54. This *Dist*$_{PC}$ value does not however, take account of two different sources of interference:

i) *co-channel* – interferers on the same channel;

ii) *adjacent channel* – interferers on channels adjacent to the PU.

For i), the DTT receiver is located on the protection contour, which for the Mendip area means *RSS*$_{PC}$ = *-86.2429*dBm. The co-channel interference signal is now increased until the BER exceeds the 2x10^{-6} threshold, which occurs at *RSS*=*-131.9*dBm. Using this value, a model was developed to determine the distance from the protection contour that would generate an interference of *-131.9*dBm at the DTT receiver. It was assumed SU BS transmit *effective isotropic radiated powers* (EIRP) of 17dBm and 4dBm [12] are used along with the TVWS

parameters defined in Table 1, 16 QAM at 32Mbps raw data (user application data together with IP and MAC overheads), and an 8MHz DTT bandwidth. This equates to a minimum keep out distance ($Dist_{KO}$) of 3.75Km from the DTT receiver on the protection contour for the 17dBm SU, while $Dist_{KO}$=1.77Km for the 4dBm SU. Both $Dist_{KO}$ distances crucially assume no margin for a hidden node.

For adjacent channel interference, the adjacent channel interference signal (*N+1*) was increased on the DTT receiver at the protection contour until the BER exceeded the $2x10^{-6}$ limit, which occurred when *RSS=-47.77*dBm. This is the maximum allowable SU signal strength in this adjacent channel. Undertaking the same analysis for the *(N+2)* adjacent channel gave a maximum *RSS=196.4*dBm for a SU.

To critically evaluate whether the OFCOM SU maximum transmit EIRP of 4dBm for *(N+1)* and 17dBm for the *(N+2)* adjacent channel interference provides sufficient DTT PU defence against interference, the SU BS and mobile scenarios where the interfering RSS is calculated for both 4dBm and 17dBm SU transmit EIRP on *(N+1)*, 14m away from a DTT receiver which is assumed to be the minimum separation of a SU BS from a PU receive antenna. The respective *(N+1)* BS results were -47.78dBm and -34.78dBm, which endorses the Ofcom decision to limit the *(N+1)* transmit EIRP to only 4dBm, as this is lower than -47.77dBm so it will not generate interference from 14m, unlike the 17dBm SU BS. The SU mobile scenario for *(N+1)* using 4dBm SU transmit EIRP gives protection to the PU receiver up to 5.4m away from the PU receiver. In contrast, for the *(N+2)* channel case, the -13dBm RSS caused by a 17dBm SU BS at 4m from the PU receiver is much lower than 196.4dBm, so no interference is generated. In the 17dBm SU mobile case, a *RSS*= -5.4dBm is generated when 1m away from the PU receiver which again is much lower than 196.4dBm, so no interference is produced to any PU.

While these co-channel results demonstrate the minimum distance away from the protection contour a SU can reliably transmit on the same channel, the *hidden node* issue [17, 34] is not reflected. It is clear from the above discussion that no interference is generated provided the Ofcom settings (Table 1) on the (*N+1)* and (*N+2)* SU power restrictions are upheld.

So far, the *hidden node* effect has been only considered in sensing a PU very close to an obstacle i.e. 10m and 20m away. The graph in Figure 18 shows the sensor output at distances more than 55Km away from a DTT transmitter, for differing obstacle heights in the range 15m to 90m [32, 33, 34]. The graph reveals that while the distance to the *keep out contour* distance varies between points (2) which are the minimum, and points (3), the maximum, depending on the obstacle height, the keep out margin X_{KO} remains constant.

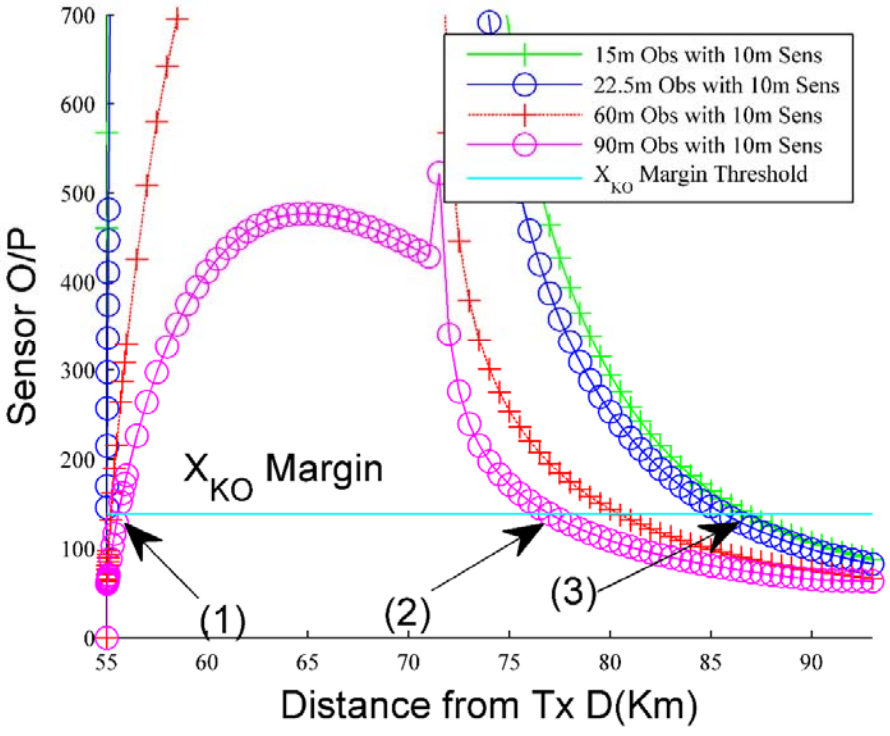

Figure 18: Mendip Keep Out Contour at 738MHz

At point (2), the minimum distance at 76.89 Km is 22.87 Km from the nearest DTT receiver ($Dist_{KO}$) on the protection contour. This means from Table 1 where the maximum allowed Ofcom transmit power is 17dBm, a minimum distance of 3.75 Km is required to avoid co-channel interference. It can then be assumed that by using the *keep out margin* X_{KO}, no interference is caused by a SU transmitter with an obstacle height of 90m. For a typical residential scenario and a 15m obstruction, the maximum *keep out contour* distance is 86.69 Km at point (3), which is the value used in channel re-use calculations. Note, the distance from the obstruction to point (1) is just 0.58 Km which represents a special case where PU detection is only achievable using either a co-operative sensing strategy or special sensor heights as discussed in [33] and needs to be within 1Km of the obstruction.

9.2 Keep out contour

This contour defines the exclusion zone around the DTT transmitter which protects the PU receiver by applying the *protection contour* even when there is a hidden node present. It also provides sufficient bandwidth to TVWS devices to ensure their users receive the best *QoS*. The difference between the protection and keep out contours is that the latter includes a margin loss alongside the protection contour to permit prescribed interference RSS in the presence of hidden nodes as illustrated in Figure 19.

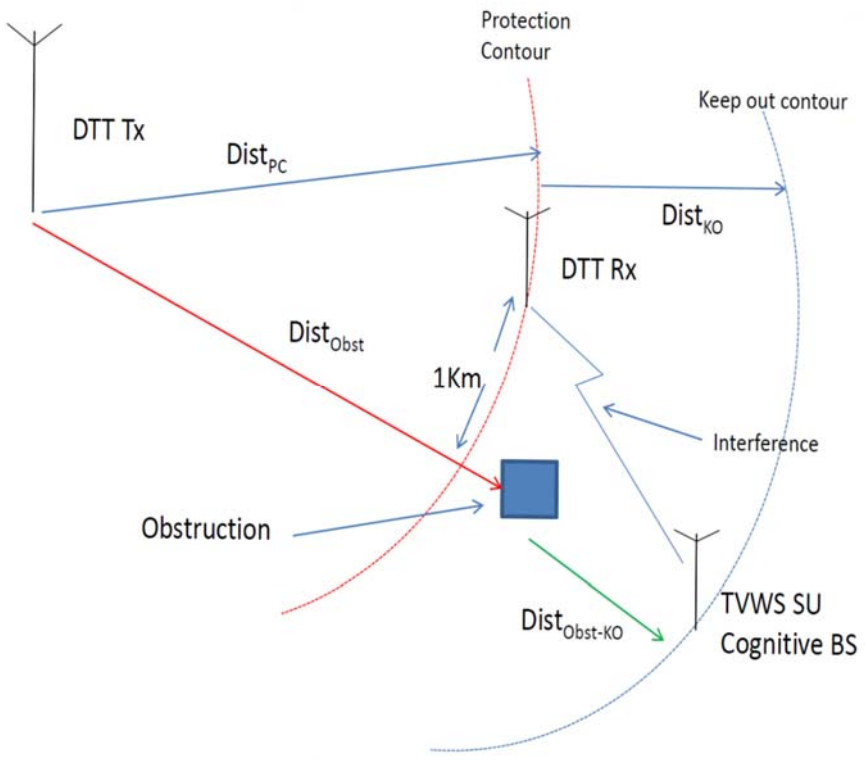

Figure 19: Keep out contour geometry

In the *keep out contour* geometry of Figure 19, the main parameters are:

Dist$_{PC}$ = *protection contour* for the lowest modulation scheme in the DTT deployment.

Dist$_{KO}$ = Distance from the *protection contour* to *keep out contour*

Dist$_{Obst}$ = Distance between an obstruction and DTT transmitter.

Dist$_{Obst-KO}$ = Distance from an obstruction to the *keep out contour*.

To define the *keep out contour*, the distance from the *protection contour* in the worst-case scenario must be determined, namely a 36dBm SU BS (maximum RF power in Table 1) producing an interference signal strength of -120.8dBm plus a margin for the hidden node. This margin is derived from the mid-variation point of the 90m obstacle diffraction loss at distances up to 400m away from an obstacle, where the most significant changes occur at 41.33dB. Using the interference models, the corresponding distance *Dist$_{KO}$* for this margin in the Mendip DTT

region is 47Km. Distance $Dist_{KO}$ + $Dist_{PC}$ now determines the minimum sensor threshold X_{KO} for the *keep out contour*. For the Mendip DTT area this is 138.73, which means any sensor output value lower than 138.73 will trigger the *keep out contour* to enable the SU to access that particular channel as shown in Figure 18.

Figure 18 reveals that while the distance to the *keep out contour* varies between the highlighted points (2) and (3), depending on the obstacle height, X_{KO} remains constant. For the most typical residential scenario and a 15m obstruction, it can be assumed the maximum *keep out contour* distance is 86.69 Km, which is the value used in channel re-use calculations. Note, the distance from the obstruction to point (1) is just 0.58 Km which represents a special case where PU detection is only achievable using either a co-operative sensing strategy or special sensor heights [33, 34].

The GEDA model employs the *keep out contour* to both determine active PU channels and to govern whether these channels can be accessed by a SU. The complete adjacent and co-channel interference management process is presented in pseudo-code form in [17], with Table 4 defining the key parameters.

Table 4: Power control parameters

X_{KO}	Keep Out Contour energy (Section 5.2)
$P_{BS(N+1)}$	Regulatory definition for base station EIRP for adjacent channel (Table 1)
$P_{BS(N+2)}$	Regulatory definition for base station EIRP (Table 1)
$P_{M(N+1)}$	Regulatory definition for mobile EIRP for adjacent channel (Table 1)
$P_{M(N+2)}$	Regulatory definition for mobile EIRP (Table 1)
DB_{PU}	GEDA identified PU Channel database
DB_{DTT}	DTT Channel database containing channel numbers and energy measurements
$DB_{DTT}^{(Ch)}$	DTT Channel database channel number
$DB_{PU}^{(Ch)}$	GEDA identified PU Channel database channel number
$DB_{DTT}^{(E)}$	DTT Channel database energy measurement

The interference management algorithm [17] checks every DTT channel in the PU database, which is created during the GEDA process, against the current channel under review. If the sensor output of the DTT under review is greater than (X_{KO}) and the channel number is specified in the PU database i.e. it is a co-channel, then a SU cannot access this particular channel. However, if the channel under review does not reside in the PU database or the sensor output is less than X_{KO}, then a SU may access the channel using RF powers of $P_{M(N+2)}$ and $P_{M(N+2)}$ respectively. Finally, if the channel under review lies in an adjacent channel *N+1* or *N+2* then the SU may use RF powers; $P_{M(N+1)}$, $P_{M(N+2)}$, $P_{BS(N+1)}$ or $P_{BS(N+2)}$ respectively, without crucially impacting upon the PU.

In [14] and [36], the available TVWS bandwidth calculation at any location was determined from physical RF surveys, which incurred extensive resources, so instead GEDA adopted the innovative strategy to assess the amount of SU bandwidth available using the *keep out contour* and so-called *sterilisation index* (SI) [33].

The UK DTT network consists of major regions, with each having minor transmitters operating within their boundaries to overcome local propagation issues so ensuring populated areas have service coverage. The USA DTT deployment in contrast has distributed major transmitter sites covering a region, though notably the *SI* concept is still applicable.

Let the *keep out contour* area of adjacent main DTT transmitters transmitting intersecting a major DTT area be F Km^2 per DTT channel per transmitter. If Y Km^2 is the area covered by the furthest *keep out contour* of a major transmitter serving a UK DTT region, then for a distributed deployment like the US, this will represent the area covered by the radius of the

furthest away transmitter *keep out contour*, added to the distance from the transmitter to the centre of the region under analysis. *SI* is thus formally expressed as:

$$SI = \frac{F}{Y} \qquad (3)$$

where the *SI* is calculated on per channel (n), per transmitter (m) basis, with each individual si_{mn} value used to construct a primary area SI' matrix.

$$SI' = \begin{pmatrix} si_{11} & \cdots & si_{1n} \\ \vdots & \ddots & \vdots \\ si_{m1} & \cdots & si_{mn} \end{pmatrix} \qquad (4)$$

where the number of DTT channels n=32 in the UK, and m the number of transmitters radiating into area *Y*. If two different transmitters use the same channel, with one *keep out contour* area nested within another, then the lower si_{mn} value is set to zero.

The final step is to sum all columns and resulting rows in equation (4) to form a final *SI* value.

$$SI = \sum_{i=1}^{n} \sum_{j=1}^{m} SI'_{ij} \qquad (5)$$

The *SI* determines the available bandwidth in the DTT area under investigation by (*N*-*SI*) x *BW* MHz, where *N* DTT channels of bandwidth of *BW* MHz area assumed in the country of interest. The next section investigates how the *SI* can be applied to determine the number of TVWS channels available in the specific case study area of the Mendip region.

9.3 UK Case Study for TVWS in the Mendip DTT transmitter area

All the major, adjacent and minor transmitters of either 50W or more (5) in the Mendip DTT transmitter area, together with their corresponding *SI* values are given in Table 5.

Table 5: Corresponding SI values for the DTT Major, Adjacent and Minor Transmitters of 50W or over

Transmitter Site	SI
Mendip	6
Wenvoe	3.495
Pontypool	0
Bristol Kings	0.36
Cirencester	0.12
Stroud	0.162
Bath	0.132
Hannington	0.942
Cerne Abbas	0.1584
Stocklands Hill	3.15
Salisbury	0.6
Bristol IC	0

Using the individual *SI* values in Table 5, the overall *SI* in (5) is 15.1194 which equates to an available bandwidth of 135MHz for TVWS SU devices, when considering all transmitters of either 50W or greater. However, there are 60 minor DTT transmitters operating below 50W that must also be taken into account. To do this efficiently, the average antennae heights and EIRP values are used to determine the *SI*. The *SI* for each channel was found to be 0.0133, and since 3 channels are allocated to each minor transmitter, $SI=2.4$. This is now added to (5) giving a total $SI=17.5194$, so the average available bandwidth for TVWS over the entire Mendip area

is 115.85MHz. While this represents the average available bandwidth for the Mendip DTT region, this value will vary according to locality. In heavily populated areas, it will reduce while in rural areas it will increase. This corroborates the findings in [13], which based on measured availability and geo-location database access, showed that in the largest city (Bristol) in the Mendip DTT region, 104MHz of bandwidth was available for TVWS devices.

Other Ofcom studies [13] suggest that over 90% of the population can access at least 100MHz, aggregated across the interleaved spectrum. They also estimated that ≈50% of the population could have access to 150MHz or greater and some rural communities could enjoy more over 200MHz of this spare capacity [17]. These findings underscore the importance the *keep out contour* threshold and *SI* play in releasing valuable bandwidth for SU TVWS exploitation, while upholding the *QoS* provision for PU DTT users. As an illustration, the SU gains secured for the Mendip region using the *SI* is approximately 6 x 20MHz LTE RF bearers per location. This translates to an increase in the number of active data users in a LTE cell location from 800 to 4600, if a TVWS access node is used in conjunction with an LTE eNodeB, i.e., an improvement of more than a factor of 5.

10. Future Research Challenges in TVWS and 5G

Emerging 5G technologies [7, 8, 9] recognise that coverage, throughput and latency are the overarching objectives in both framing and advancing any new wireless standard. This chapter has presented a flexible framework for how TVWS can effectively fulfil some of these aims by enabling 5G services to not only utilise the increased spectrum released by TVWS, but also safeguard long-term access benefits for unlicensed SU.

Central to this novel TVWS access framework is the GEDA model which uniquely depends on the DTT channel deployment patterns. It is thus motivated by the narrowband nature of DTT UHF receiver antenna, which means only a narrowband of channels are allocated to a specific region. To exploit the SU access benefits of GEDA in other spectrum opportunities such has the millimetre spectrum, it will need to be modified to be able to detect other patterns, such as timing of the PU signals or when new spectrum is allocated to a PU by administrators, such patterns are factored into the allocation.

Another key challenge is to improve the SU transport QoS metrics of *packet error rate* (PER) and latency when accessing TVWS. Existing TVWS regulatory requirements [13] mean SU BS transmits at far higher RF power compared to SU mobile units, so to achieve adequate SU coverage, the uplink signal from the mobile device to BS needs to employ newly developed innovative routing models to achieve the additional coverage through multi-hop network arrangements.

Furthermore, heterogeneous network environments have been introduced to access different technologies to meet user requirements. An underlying assumption of this development is that TVWS spectrum would be shared between multiple mobile operators, with each setting up a separate WLAN. An interesting alternative strategy would be to critically investigate open WLAN arrangements, involving some commercial agreements between operators for resource sharing [37]. Multi-operator heterogeneous networks have the advantage that any mobile operator can route packets so increasing the number of mobiles in a routing area because it is not restricted to one operator. This will increase the mobile routing population in an area so reducing the PER. A major research question for such an environment however, would be how

best to create a cross-operator heterogeneous implementation framework on existing platforms, including the cognitive TVWS access framework presented in this chapter.

11. Conclusion

This chapter has investigated how *cognitive radio* (CR) technologies can address the scarcity of spectrum for the increasing demands made by today's wireless applications. It in particular, explores how *TV White Space* (TVWS) offers a unique, low-risk option to enhance existing licensed spectrum by exploiting unlicensed resources due to the static temporal characteristics of the *primary user* (PU) spectrum. The key hurdles to TVWS adoption are reliable PU detection allied with resolving the *hidden node* issue. A review of existing TVWS regulatory standards has been presented with the PU-centric country related requirements detailed together with the SU-centric requirements. A key conclusion is that any proposed sensing solution needs to robustly demonstrate resilience to the omnipresent *hidden node* problem.

Supporting technologies which facilitated the introduction of CRN including cross-layer processing and ad-hoc routing were also reviewed to address the challenges of both supporting SU access to TVWS and overcoming latency issues of ensuring the correct information is delivered to the required OSI layers in a timely fashion. Ad hoc routing has been highlighted as the favoured solution for ensuring the unidirectional transmission caused by the SU RF power differentials, do not negatively impact on user QoS.

Finally, PU interference management has been analysed with a novel *Generalised Enhanced Detection Algorithm* (GEDA) detailed which exploits the unique way *Digital Terrestrial TV* (DTT) channels are deployed in different geographical areas. GEDA transforms an energy detector into a feature sensor to achieve significant sensing improvements compared to existing detection solutions. By applying a *keep out contour* together with a novel *sterilisation index*,

the *hidden node* problem is resolved, and a practical SU sensing solution formulated. GEDA and the *keep out contour* interference management paradigm leverages extra bandwidth for SU in TVWS to achieve notably enhanced QoS provision as demonstrated in a UK DTT transmitter case study. The advantages of GEDA has also been shown to be equally effective in DTT deployments in other countries.

References:

[1] Cisco (2016) *Cisco Visual Networking Index: Global Mobile Data Traffic Forecast Update, 2015 – 2020* [Online], Available at http://www.cisco.com/c/dam/m/en_in/innovation/enterprise/assets/mobile-white-paper-c11-520862.pdf (Accessed February 2016).

[2] Hossain, E. and Niyato, D., Han, Z. (2009) *Dynamic Spectrum Access and Management in Cognitive Radio Networks*, Cambridge UK, Cambridge University Press.

[3] Nekovee, M. (2010) 'Cognitive Radio Access to TV White Spaces: Spectrum Opportunities, Commercial Applications and Remaining Technology Challenges', *IEEE DySPAN*, Singapore, 6-9 April 2010, USA, IEEE, pp. 1-10.

[4] Fitch, M., Nekovee, M., Kawade, S., Briggs, K., MacKenzie, R. (2011) 'Wireless service provision in TV white space with cognitive radio technology: A telecom operator's perspective and experience', *IEEE Communications Magazine*, vol. 49, no. 3, pp. 64-73.

[5] OFCOM (2016) *Digital Switchover Transmitter Details* [Online]. Available at https://www.ofcom.org.uk/spectrum/information/transmitter-frequency (Accessed 14th Mar 2017).

[6] FCC (2015), *Engineering DTV Maps* [Online], Available at https://www.fcc.gov/media/engineering/dtvmaps (Accessed January 2015).

[7] GSMA (2014), *Understanding 5G: Perspectives on future technological advancements in mobile* [Online]. Available at https://www.gsmaintelligence.com/research/?file=141208-5g.pdf&download (Accessed February 2016).

[8] NGMN (2015), *NGMN 5G White Paper*, Frankfurt Germany, NGMN, Version 1.0.

[9] EPRS (2016), *5G network technology- Putting Europe at the leading edge*, Brussels, European Parliament, PE 573.892.

[10] Akyildiz, I F., Lee, W-Y., Chowdhury, K R. (2009) 'CRAHNs: Cognitive radio ad hoc networks', Network IEEE vol.23 no. 4, pp 6—12.

[11] Haykin, S. (2005) 'Cognitive radio: Brain empowered wireless communication', *IEEE JSAC*, vol. 23, no. 2, pp. 201-220.

[12] Nekovee, M. (2011) 'Current Trends in Regulation of Secondary Access to TV White Spaces Using Cognitive Radio', *IEEE Globecom 2011*, Kathmandu Nepal, 5-9 Dec 2011, USA, IEEE, pp. 1—6.

[13] Nekovee, M. (2012), *TV White Space Services in the UK: Current Status and Future*

Directions, BT, HSN 2012 Conference presentation 12/1/2012 Jeju Island, South Korea.

[14] Cambridge White Spaces Consortium (2012), *Cambridge TV White Spaces Trial, A Summary of the Technical Findings* [online]. Available at http://www. cambridgewireless.co.uk/docs/Cambridge (Accessed 20th April 2013).

[15] Chen, K-C. and Prasad, R. (2009), *Cognitive Radio Networks*, Chichester UK, Wiley

[16] Akyildiz, I F., Lee, W-Y., Vuran M C., Mohanty, S. (2006) 'NeXt generation/dynamic spectrum access/cognitive radio wireless networks: A survey', Computer Networks vol. 50 pp. 2127–2159.

[17] Martin, J H., Dooley, L S., Wong, K C P. (2016) 'A New Dynamic Spectrum Access Algorithm for TV White Space Cognitive Radio Networks', *IET Communications Journal*, vol. 10, no.18, pp. 2591 – 2597.

[18] OFCOM (2015), *Implementing TV White Spaces*, London UK, OFCOM, 12 February 2015.

[19] Ramjee, R., Roy, S., Chintalapudi, K. (2016) 'A critique of FCC's TV white space regulations', GetMobile, vol. 20, no. 1, pp. 20-25.

[20] Nominet (2018) Autonomous Vehicles [Online]. Available at https://www.nominet.uk/emerging-technology/autonomous-vehicles-driven/ , (Accessed February 2018).

[21] Lei Qiu Jing, C., Viessmann, A., Kocks, C., Bruck, G H., Jung, P., Qingyang Hu, R. (2011) 'A Spectrum Sensing Prototype for TV White Space in China', *GLOBECOM 2011*, Kathmandu Nepal, 5-9 Dec. 2011, USA, IEEE, pp. 1—6.

[22] Chen, H-S. and Gao, W. (2011),'Spectrum Sensing for TV White Space in North America', *IEEE Journal on selected areas in communications*, vol. 29, no. 2, pp 1—11.

23] IEEE (2013) 802.11af™-2013: *IEEE Standards- Amendment 5: Television White Spaces (TVWS) Operation*, USA, IEEE Computer Society.

[24] Sheng, L., Shao, J., Ding, J. (2010) 'A Novel Energy-Efficient Approach to DSR Based Routing Protocol for Ad Hoc Network', *ICECE 2010*. Wuhan China, 25-27 June 2010, USA, IEEE, pp. 2618 – 2620.

[25] Yuanzhou, L. and Weihua, H. (2010) 'Optimization Strategy for Mobile Ad Hoc Network Based on AODV Routing Protocol', *WiCOM 2010*, Chengdu China, 23-25 Sept. 2010, USA, IEEE, pp. 1-4.

[26] Baldo, N. and Zorzi, M. (2008) 'Fuzzy Logic for Cross-layer Optimization in Cognitive Radio Networks', *IEEE Communications Magazine*, vol. 46, no. 4, pp. 64—71.

[27] Mitola, J. and Maguire, G Q. (1999) 'Cognitive Radio: Making Software Radios More Personal', *IEEE Personal Communications*, vol. 6, no. 4, pp. 13—18.

[28] Ghosh, C. and Agrawal, D P. (2007) ’ROPAS: Cross-layer Cognitive Architecture for Wireless Mobile Adhoc Networks’, *IEEE International Conference on Mobile Adhoc and Sensor Systems*, Pisa Italy, pp 1—7.

[29] Kokar, M M. and Lechowicz, L. (2009) ‘Language Issues for Cognitive Radio’, *Proc. of IEEE*, vol. 97, no. 4, pp. 689—707.

[30] He, A., Bae, K K., Newman, T R., Gaeddert, J., Kim, K., Menon, R., Morales-Tirado, L., Neel, J., Zhao, Y., Reed, J H., Tranter, W H. (2010) ‘A Survey of Artificial Intelligence for Cognitive Radios’, IEEE Transactions on Vehicular Technology, vol. 59 no. 4, pp. 1578—1592.

[31] Zhu, X., Champagne, B., Zhu, W-P. (2013) ‘Cooperative Spectrum Sensing Based on the Rao Test in Non-Gaussian Noise Environments’, *WCSP 2013*, Hangzhou China, 24-26 Oct. 2013, USA, IEEE, pp. 1-6.

[32] Martin JH, Dooley LS, Wong KCP, (2011), A New Cross-Layer Design Strategy for TV White Space Cognitive Radio Applications, IEEE IWCLD, pp 1—5

[33] Martin JH, Dooley LS, Wong KCP, (2013) A New Cross-Layer Dynamic Spectrum Access Architecture for TV White Space Cognitive Radio Applications, IET ISP, pp 1—5

[34] COGEU (2009), *Cognitive radio systems for efficient sharing of TV white spaces in European context* [Online]. Available at http://www.ict-cogeu.eu/pdf/COGEU_D2_1%20(ICT_248560).pdf (Accessed 20th April 2015).

[35] Herbert Taub, Donald L. Schilling (1986). *Principles of Communication Systems.* McGraw-Hill.

[36] Kyu-Min Kang, Jae Cheol Park, Sang-In Cho, Byung Jang Jeong (2012), Deployment and Coverage of Cognitive Radio Networks in TV White Space, IEEE Communications Magazine, December 2012.

[37] Alcatel-Lucent and BT (2013) *WI-FI ROAMING – BUILDING ON ANDSF AND HOTSPOT2.0* [Online]. Available at http://www.tmcnet.com/tmc/whitepapers /documents/whitepapers/2013/6686-wi-fi-roaming-building-andsfand-hotspot20.pdf, (Accessed July 2015).